## DELFT UNIVERSITY OF TECHNOLOGY

# Experiment Design for Parameter Estimation of Individual Motion Sickness Dynamics

Author: Martijn Mooi (4578538)

Master of Science Mechanical Engineering, Track: Vehicle Engineering

> Supervisors: Riender Happee Tuğrul Irmak

October 30, 2023



## Abstract

In the near future, travelling in vehicles will no longer be in regular vehicles, but in automated vehicles. The share of automated vehicles is predicted to increase significantly within 20 years. Passengers in automated vehicles will engage in non-driving tasks, such as sleeping, reading, working or just otherwise spending time on their phone. This will result in motion sickness becoming more prevalent, as passengers will no longer pay attention to the road. Therefore, there is a need for research in motion sickness. To further our understanding of motion sickness and possible mitigation strategies, mathematical models of motion sickness need to be developed. The temporal dynamics of motion sickness can be captured in the so called 'Oman model' [Oman, 1990. However, most literature use group averaged parameters and motion sickness incidence to describe motion sickness. These methods do not capture well enough how individuals respond to sickening stimuli, as recent studies showed that individuals have strongly varying responses to various frequencies. Only, estimating individual motion sickness parameters is costly thus far, requiring multiple experiments to estimate the parameters. This study explains an optimal experiment design, where the input is varied in real-time closed loop manner such that the information content in the input is maximized for estimation of parameters, rusulting in the fact that individual motion sickness parameters could be estimated in a single experiment. Results show that on average, within the first 63 minutes, most parameter estimations have converged. The resulting RMSE is 1.06 on the MISC scale, comparing to other literature. This shows that the frequency and temporal dynamics of motion sickness and an individual level can be estimated at a drastically faster rate than previous methods. To our knowledge this is the first use of optimal experiment design techniques to asses the dynamics of human responses to stimuli in general, which is an important milestone for cybernetics research.

Keywords – Motion Sickness, Modelling, Parameter Estimation, Experiment Design

# Contents

1	Intr	roduction	3
2	Est	imation Method	7
	2.1	The Oman Sickness Model	7
	2.2	Optimal Experiment Design	
	2.3	Error Metrics	11
	2.4	Performance of the Simulation	14
3	Met	thodology	16
	3.1	Ethics Statement	16
	3.2	Participants	16
	3.3	Apparatus	16
	3.4	Briefing	18
	3.5	Experiment	18
		3.5.1 Sickness Metrics	18
		3.5.2 Procedure	19
	3.6	Data Analysis	20
		3.6.1 Convergence	20
		3.6.2 Statistical Analysis	21
4	Res	ults	22
	4.1	Course of the Experiment	22
	4.2	Statistical Analysis	
	4.3	Duration of Estimation	
	4.4	Estimation of Parameters	24
5	Disc	cussion	27
	5.1	Performance of the Algorithm	27
	5.2	Limitations	28
		5.2.1 Q Parameter	28
		5.2.2 Processing Power	29
		5.2.3 Simulator Limits	30
	5.3	Previous Literature	31
6	Cor	nclusion	32
7	Ack	nowledgements	32
		nces	33

A	MSSQ	35
В	MISC	36
$\mathbf{C}$	Convergence of Parameters	37

## 1 Introduction

.

Fully automated vehicles will become a reality in the near future. It is expected that by 2040 the market share of fully automated vehicles of SAE level 3-5 [SAE International, 2014 will reach 20-40% [Litman, 2022]. These automated vehicles are designed to improve the safety of passengers and the traffic, as driver error is the cause of 94% of motor-vehicle crashes [Singh, 2018], and automated vehicles could prevent 34% of crashes [Mueller et al., 2020]. Additionally, automated vehicles can improve travel comfort with adaptation of control strategies to maximize comfort. Passengers will be able to do non-driving related tasks during their journeys, but in doing so, their eyes are not focused on the road. When passengers do not have their eyes on the road ahead, motion sickness will develop both more frequently and faster [Diels and Bos, 2015], meaning that with the increase of automation, motion sickness will also be more prevalent among road users [Diels and Bos, 2015. This is not the case for the driver as the driver of the vehicle does not get motion sick. However, the driver will become the passenger as well in automated vehicles. The development in motion sickness therefore will be a big hurdle to overcome in the acceptance of automated vehicles, as when passengers get sick during their travels, they are less likely to adopt the technology.

This is why a good understanding of motion sickness is necessary. The understanding of motion sickness allows us to describe the development of the symptoms and model the dynamics of motion sickness development. When motion sickness can be modelled, the designers of automated vehicles are better equipped to address the problem. The designers could implement novel control strategies in the vehicle to prevent or reduce motion sickness, and develop methods, which for instance, warn the passenger of oncoming manoeuvres, allowing passengers to anticipate movements, and thus reducing motion sickness [Kuiper et al., 2020].

Motion sickness is a complex syndrome, where nausea and vomiting are the main symptoms, and it affects a wide range of species. Symptoms also include sweating, headaches, dizziness, drowsiness, stomach awareness, pallor, increased salivation, hyperventilation and belching [Bertolini and Straumann, 2016]. Around one-third of the population is highly susceptible [Takov and Tadi, 2019], while most of the population experiences motion sickness with sufficient inertial-motion cues. People can also experience visually induced motion sickness [Keshavarz et al., 2014]. The motion sickness susceptibility differs a lot between individuals, with ratios up to 10,000 to 1 [Lackner, 2014], where there are different factors which predict the susceptibility of motion sickness, with the main predictors being sex and age [Golding, 2016a]. When the sickening motions sustain for a longer period

of time, subjects can develop sopite syndrome, which has symptoms including lethargy and drowsiness [Graybriel and Knepton, 1976]. This has a negative effect on the cognitive performance when multitasking, meaning passengers could have a declining performance when performing non-driving related tasks [Smyth et al., 2018, Matsangas et al., 2014], which is one of the main benefits of automated vehicles versus non-automated vehicles. Thus, motion sickness could prevent a large portion of the population from benefitting from the advantages of automation, and disregarding the technology for cheaper alternatives, such as regular vehicles.

An important mechanism in the genesis of motion sickness is the vestibular system, which provides humans with a sense of balance and spatial orientation. The information from the vestibular system is used for coordinating movement with The vestibular system consists of two components: the semicircular canals and the utricle and saccule. The semicircular canals consist of three canals in different planes, which can sense angular acceleration and rotation of the head. The utricle and saccule are sensitive to linear acceleration, gravitational forces and tilting of the head. The utricle and saccule contain otoliths, which sense the forces resulting from acceleration. The signals of the vestibular system are essential to the onset of motion sickness. Subjects who have complete bilateral loss of labyrinthine function, meaning they have no vestibular sense organs, are immune to motion induced motion sickness [Golding, 2016b]. Interestingly however, they are not immune to visually induced motion sickness, it is thought that this could be due to the remanence of residual vestibular function [Golding, 2016b], or triggering the same mechanisms as regular motion sickness, as visual and physical acceleration appear to share the a sensory integration process which results in motion sickness.

This study focuses on the sensory conflict model for motion sickness, as this theory has a mathematical basis needed to model the dynamics of motion sickness. For example, the postural instability theory does not have models to model the dynamics of motion sickness [Riccio and Stoffregen, 1991, Stoffregen and Smart, 1998]. The neural mismatch theory, a predecessor of the sensory conflict theory, was first developed by Reason [Reason, 1978]. The neural mismatch theory states that all situations which provoke motion sickness are characterized by a condition of sensory rearrangement in which the motion signals transmitted by the eyes, the vestibular system and the nonvestibular proprioceptors are at variance with one another, and hence with what is expected on the basis of previous transactions with the spatial environment. The theory also adds that, in order for motion sickness to develop, the vestibular system is essential, as is discussed earlier in this section. This theory was later expanded on and mathematically supported by

Oman [Oman, 1990], resulting in the sensory conflict theory. This mathematical model then formed the basis for modelling motion sickness responses of individuals and groups in modern research [Irmak et al., 2021, Kotian et al., 2023].

There are multiple studies which try to model the motion sickness development. Most studies use a measure of motion sickness incidence (MSI), which only captures the percentage of the subjects that vomit due to the applied accelerations. This method does not capture the dynamics of motion sickness development, as it is preferred to keep passengers far below the level of vomiting when travelling with an automated vehicle. Thus, only a knowledge of the MSI does not suffice for adaptation of control to prevent motion sickness.

Furthermore, most studies which try to model the motion sickness dynamics, only average over the group when fitting the models. It is shown that individuals respond differently to motion cues, mainly the frequency where the sickening effect peaks [Irmak et al., 2021]. To individualize the adaption of an automated vehicle to a passenger, knowledge about the passenger's motion sickness dynamics is required. The goal of this research is thus to capture the individual motion sickness dynamics using a relatively short experiment. Currently, data collection methods used are time-consuming and expensive, for example spanning four experiments of 105 minutes (maximum) [Irmak et al., 2022]. This creates a data bottleneck. Capturing the individual motion sickness dynamics can be done using optimal experiment design, which this report explains and implements in an experiment to estimate individual motion sickness parameters.

The modelling of the temporal dynamics of motion sickness at an individual level will grant more insight in the concept. When understanding the differences in motion sickness dynamics of the individual, more measures can be researched in preventing or minimizing motion sickness. This will lead to more comfort in travel, as the knowledge about the temporal dynamics of motion sickness can be applied to more modes of transport, granted there is research in the different motion cues and how it affects motion sickness. This could lead to a more practical implementation in automated vehicles, where the vehicle could estimate the sickness parameters of the passengers inside, and subsequently adapt its control strategy to improve the travel comfort of the passengers. Furthermore, this experiment is done in a driving simulator. This affects how motion sickness develops [Talsma et al., 2023]. However, together with the research on the difference in simulator sickness versus motion sickness, this research will have a meaningful impact in the understanding of the temporal dynamics of motion sickness for the individual.

To summarize, the goal of this research is to design a method to estimate the mo-

tion sickness parameters of individuals using optimal experiment design. Based on literature and successful simulation, the effectiveness of the method is tested using human participants. Using the literature and simulations, it is hypothesized that:

- The estimation method estimates the parameters within one session of a maximum of 1.5 hours.
- The model using the estimated parameters will predict the MISC rating of individuals with an accuracy of 0.5 on the MISC scale, as from simulations the RMSE was lower than 0.5 on average.
- Not all parameters need to converge, as not all the parameters are as important for a good fit. This means convergence of the model does not necessarily result in convergence of all the model parameters.

In the subsequent sections, the estimation method is explained, followed by the detailing of the experiment method. Then, the results of the experiment are shown and consequently discussed. Last, conclusions are taken from the results.

#### 2 Estimation Method

This section details the method used to estimate the individual sickness parameters. First, the Oman model used to predict motion sickness is presented. Then, the method of estimating the parameters of the model using optimal experiment design is explained.

The estimation method is based on Optimal Experiment Design, where an input is selected based on the information content it contains with respect to the parameters of the model. This uses the Fisher information matrix, where the differential equations of the model are differentiated with respect to the parameters of the model, as seen in [Jauberthie et al., 2005]. Then, the parameters of the model are updated with the *fmincon* algorithm from MATLAB using the input and output data. These updated parameters provide an updated information matrix and thus a new input is selected.

#### 2.1 The Oman Sickness Model

First, there are two main groups of models describing motion sickness. These are functional models and descriptive models [Kufver and Förstberg, 1999]. Functional models are based on the sensory conflict theory, described in Section 1. They describe the genesis of the conflict signal which then results in motion sickness. Descriptive models make use of mathematical models to fit experimental data and therewith describe motion sickness.

Oman first made a functional model, described in Section 1. This model explained the genesis of the conflict signal based on the CNS comparing sensed motion with predicted motion. This created a mathematical framework for a model which can use equations to model motion sickness. For the modelling of motion sickness dynamics, Oman created a model which has the sensory conflict signal as input and the nausea magnitude as output, as seen in Figure 1. This model is a descriptive model, as it can adapt its parameters to data gathered from experiments.

The model has a slow path and a fast path, where the fast path models the faster onset of motion sickness due to neuronal responses, and the slow path models the slower hormonal response. The fast and slow path are both described by second order transfer functions 1 (where the top transfer function is the fast path and the bottom transfer function is the slow path). This structure can capture temporal dynamics of motion sickness as well as the phenomenon of hypersensitivity [Oman, 1990]. This describes hypersensitivity, which is the fact that individuals have a heightened sensitivity to motion cues after earlier exposure to sickening motion. Thus far, this is the only model which adequately captures hypersensitivity.

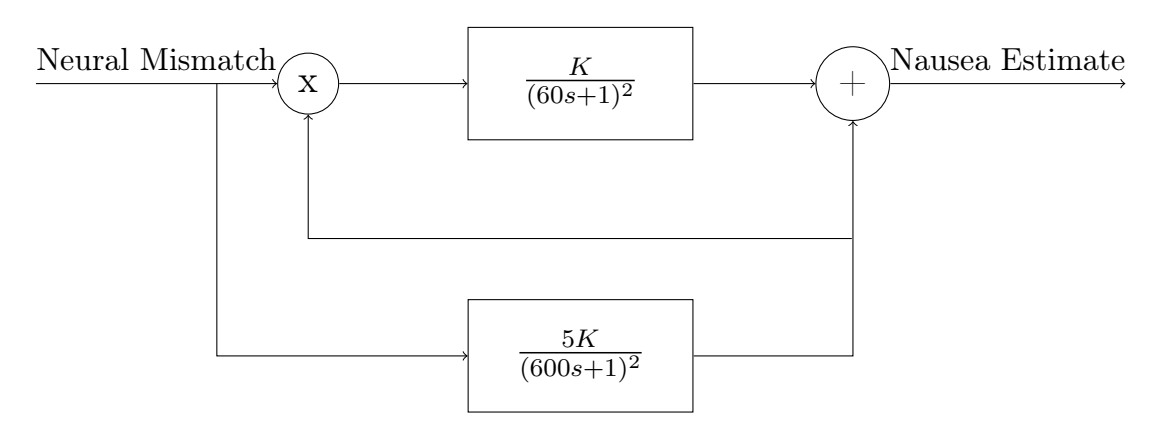


Figure 1: The descriptive Oman model [Oman, 1990]

Then for this experiment, the descriptive Oman model is adapted to model the frequency sensitivity in individuals. The frequency sensitivity is modeled as a band pass filter on the input acceleration signal. This acts to map the accelerations to a value proportional to the sensory conflict which we cannot measure. The band pass filter has a peak at the frequency the human is most sensitive to. The band pass filter can be seen in Formula 1.

$$B = \frac{\frac{\omega_0}{Q}s}{s^2 + \frac{\omega_0}{Q}s + \omega_0^2} \tag{1}$$

Where Q is the quality factor, determining the width of the peak of the filter, which is set to 0.3 to model the 'peakyness' of the filter. This value ensured that the frequency where the individual is most sensitive to evokes a response of a higher magnitude, while also still being sensitive to the other frequencies in the band. Fixing the value of Q means there is one less parameter to identify, and also requiring less computational power needed to differentiate the system equations to Q as well, ensuring that the algorithm can operate closed loop in real time. The parameter Q can also be identified after the experiment if possible, identifying if individuals are sensitive specific to a frequency or sensitive to all frequencies in the band where motion sickness occurs. The parameter which needs to be identified is  $\omega_0$ , which is the frequency the human is most sensitive to. Then, as seen in Figure 1, the model has a fast and slow path, seen in Formula 2 and 3 respectively.

$$F = \frac{K}{(\beta_1 s + 1)^2} \tag{2}$$

$$S = \frac{1}{(\beta_2 s + 1)^2} \tag{3}$$

 $\beta_1$ ,  $\beta_2$  and K are the parameters which have to be identified in the fast and slow path. The final model will have a structure as seen in Figure 2

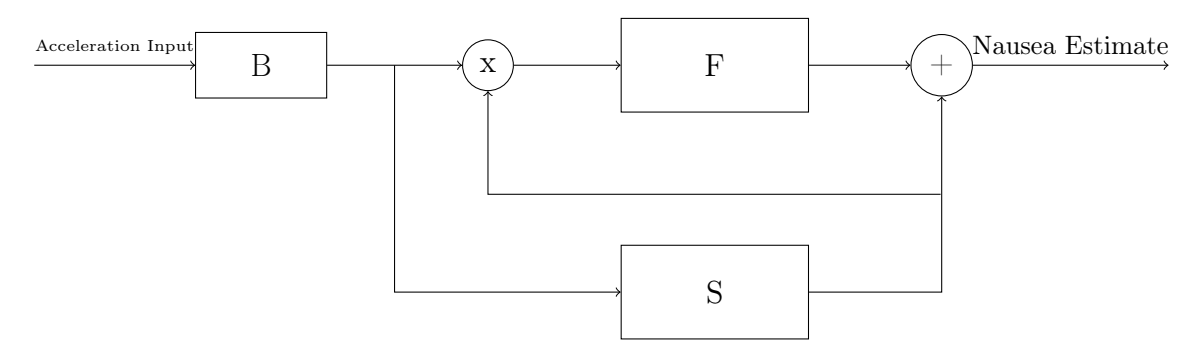


Figure 2: The final Oman model

In the model, it can be seen that the model is simplified without power law to simplify the estimation process. In the code, the input is rectified.

## 2.2 Optimal Experiment Design

[Qian et al., 2016] provides an experiment design based on economic model predictive control (EMPC). Traditional model predictive control (MPC) is a widely used strategy to track a set point for large multivariable systems subject to constraints [Rawlings et al., 2012]. In contrast, EMPC can follow the economic performance of a system rather than a set point better suited for systems which have dynamic economic performance, thus changing demands of the performance of the system. [Ellis et al., 2014] validated the stability and performance of EMPC, but noted the high computational cost of EMPC. This is not important for this case, as the computational cost is not very high for the relatively simple Oman model (Figure 2) combined with large sampling times of 30 seconds, this will later be explained in the final design of the experiment.

The EMPC algorithm has a cost function with two parts: the sensitivity criterion and the stability criterion. The sensitivity criterion is to optimize the richness of information in the inputs to accurately estimate parameters, whereas the stability criterion ensures the stability of the system. The stability criterion could model the divergent sickness responses of subjects, where the MISC rating would increase very fast in subjects (seen in [Bock and Oman, 1982] and [Irmak et al., 2020]).

However, the stability criterion of this method required an observer design which could not be made using the Oman model, as the parameters appear non-linearly in the state equations, which prevented designing the system matrices. Therefore, the input selection is based on the sensitivity criterion of the method.

To estimate the parameters, a prediction model is used for predicting the output. This prediction is based on the differential equations of the system. These differential equations of the prediction model are differentiated with respect to the parameters to obtain the sensitivities. After normalizing the sensitivities, the sensitivity matrix is created. To construct the sensitivity criterion cost function, the minimal and maximal eigenvalue of the sensitivity matrix are used, seen in Formula 4.

$$J_{\theta}(l) = \left| \frac{\lambda_{min}(M(l))}{\lambda_{max}(M(l))} \right| \tag{4}$$

$$M(l) = ||\bar{y}_{\theta}(l)||^2, l \in [k \ k + N_p]$$
(5)

$$\bar{y}_{\theta}(l) = \begin{bmatrix} \bar{y}_{1\theta_1} & \bar{y}_{1\theta_2} & \dots & \bar{y}_{1\theta_q} \\ \bar{y}_{2\theta_1} & \ddots & & \vdots \\ \vdots & & \ddots & \vdots \\ \bar{y}_{p\theta_1} & \dots & \dots & \bar{y}_{p\theta_q} \end{bmatrix}$$

$$(6)$$

Where  $\bar{y}_{\theta}(l)$  is the sensitivity matrix at timestep k, and future timestep l over the prediction horizon  $N_p$ . In the sensitivity matrix, the p outputs of  $\bar{y}$  are derived with respect to q parameters.

The sensitivity matrix is calculated differentiating the differential equations with respect to the parameters. To be able to differentiate the model with respect to the parameters, the transfer functions of the Oman model have to be transformed to the time domain using the inverse Laplace transform. The transformation will be split up into the slow path, the fast path and the band pass filter.

$$O_b = \frac{u\frac{\omega_0}{Q}s}{s^2 + \frac{\omega_0}{Q}s + \omega_0^2} \tag{7}$$

$$O_s = \frac{u}{(\beta_2 s + 1)^2} \tag{8}$$

$$O_f = \frac{uO_sK}{(\beta_1s+1)^2} \tag{9}$$

Which then result in the following differential equations:

$$\ddot{O}_b = \frac{\omega_0}{Q}\dot{O}_b + \omega_0^2 O_b \tag{10}$$

$$\beta_2^2 \ddot{O}_s = -2\beta_2 \dot{O}_s - O_s + u \tag{11}$$

$$\beta_1^2 \ddot{O}_f = -2\beta_1 \dot{O}_f - O_f + uO_s K \tag{12}$$

To calculate the sensitivity matrix from the differential equations, the differential equations have to be differentiated with respect to the parameters. The output of the system is in the form of  $O_f + O_s$  from equations 12 and 11, as seen in Figure 2. The input in the differential equations is  $O_b$  from equation 10. The equation then results in:

$$y = KO_b(O_b - \beta_2^2 \ddot{O}_s - 2\beta_2 \dot{O}_s) - \beta_1^2 \ddot{O}_f - 2\beta_1 \dot{O}_f + O_b - \beta_2^2 \ddot{O}_s - 2\beta_2 \dot{O}_s$$
 (13)

With  $O_b$  from equation 10. Then, the partial derivatives of y with respect to  $\omega_0$ ,  $\beta_1$ ,  $\beta_2$  and K are taken to compose the sensitivity matrix as seen in equation 6.

$$\frac{\partial y}{\partial \beta_1} = -2\beta_1 \ddot{O}_f - 2\dot{O}_f \tag{14}$$

$$\frac{\partial y}{\partial \beta_2} = -2\beta_2 \ddot{O}_s O_b - 2K\dot{O}_s O_b - 2\beta_2 \ddot{O}_s - 2\dot{O}_s \tag{15}$$

$$\frac{\partial y}{\partial K} = O_b^2 - \beta_2^2 \ddot{O}_s O_b - 2\beta_2 \dot{O}_s O_b \tag{16}$$

$$\frac{\partial O_b}{\partial \omega_0} = -\frac{\dot{u}}{\omega_0^2} + \frac{2\ddot{O}_b}{\omega_0^3} + \frac{\dot{O}_b}{Q\omega_0^2} \tag{17}$$

$$\frac{\partial y}{\partial \omega_0} = 2KO_b \frac{\partial O_b}{\partial \omega_0} - K\beta_2^2 \ddot{O}_s \frac{\partial O_b}{\partial \omega_0} - 2K\beta_2 \dot{O}_s \frac{\partial O_b}{\partial \omega_0} - \frac{\partial O_b}{\partial \omega_0}$$
(18)

After the sensitivity matrix is calculated, the input is selected from a range of frequencies between 0.05 and 0.55 Hz with intervals of 0.0611 Hz (10 frequencies in the band), as in this band subjects are susceptible to the sickening motion [O'Hanlon and McCauley, 1974].

Thereafter, the parameters of the model are estimated using the *fmincon* algorithm from MATLAB. The amplitude of the input is scaled in relation to the estimated gain of the model to ensure a response from individuals who are less sensitive to motion cues, and to prevent sensitive individuals to get motion sickn too fast.

#### 2.3 Error Metrics

To estimate the parameters using the *fmincon* algorithm, an error metric needs to be used to determine the goodness of the fit to compare different estimations. To see how different parameters affect the distinction between errors within error metrics, a simple script was created to simulate the Oman model multiple times

using different sets of parameters. These simulations using different sets of parameters were compared to a simulation using one control set of parameters to see what the error distribution is over all the sets of parameters. This is to see how the magnitude of errors differ when comparing the set of parameters equal to the control set of parameters, to the other sets of parameters not equal to the control set of parameters. The band-pass frequency and the slow-pass time constant were varied and the gain and the fast-pass time constant were kept constant to see the difference in errors. The varied frequencies and time constants can be seen in equations 19 and 20.

$$\omega_0 = 2 * \pi * [0.05, 0.1, 0.15, 0.2, 0.25, 0.3, 0.35, 0.4, 0.45, 0.5, 0.55, 0.6]$$
 (19)

$$\beta_2 = [300, 400, 500, 600] \tag{20}$$

Thereafter, two error metrics were compared. The symmetric mean absolute percentage error (SMAPE) and the root mean squared error (RMSE). The SMAPE is used earlier in motion sickness error estimation [Irmak et al., 2020]. The RMSE is a commonly used absolute error metric, which could be more distinctive because it is not a percentage error. The formulas for the SMAPE and RMSE can be found in equations 21 and 22.

$$SMAPE = \Sigma \left| \frac{ObservedMISC - PredictedMISC}{ObservedMISC + PredictedMISC} \right|$$
 (21)

$$RMSE = \sqrt{\frac{1}{n} \sum_{i=1}^{n} \left( PredictedMISC - ObservedMISC \right)^{2}}$$
 (22)

The parameters used for the observed MISC are  $[0.4 * 2 * \pi, 4, 40, 400]$ . As discussed earlier, the gain and the fast-pass time constant are kept constant for the predicted MISC (thus at 4 and 40). The heatmaps of the errors are created and can be seen in Figure 3 and 4.

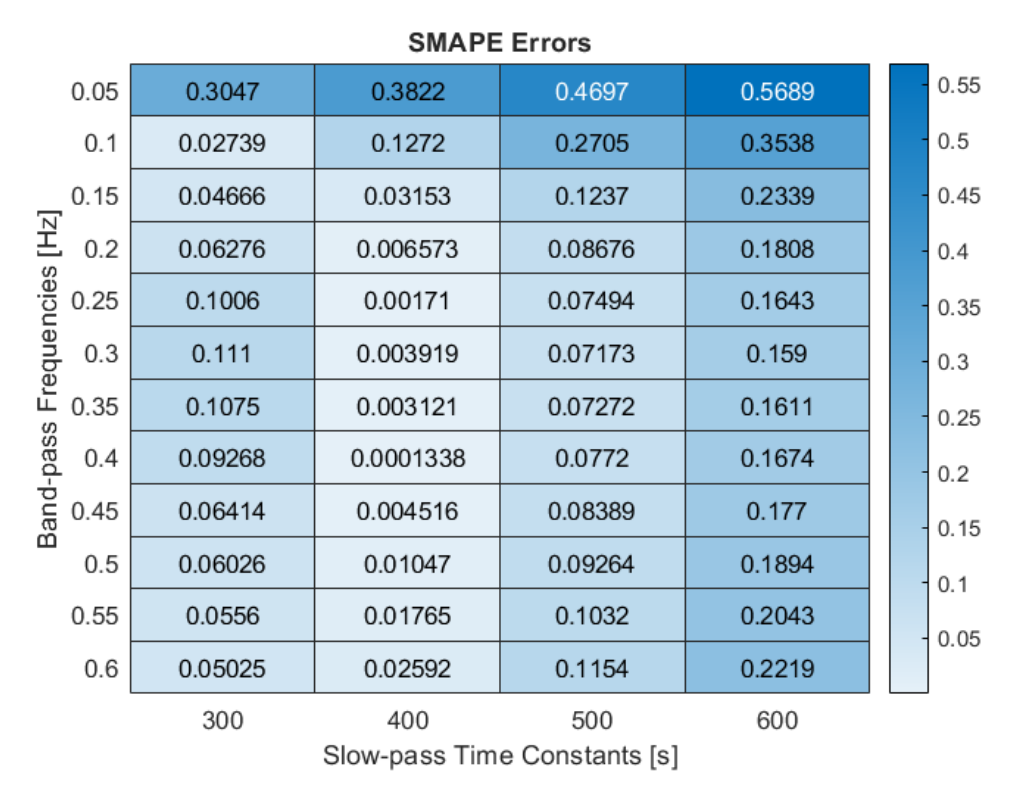


Figure 3: The heatmap of the errors using SMAPE

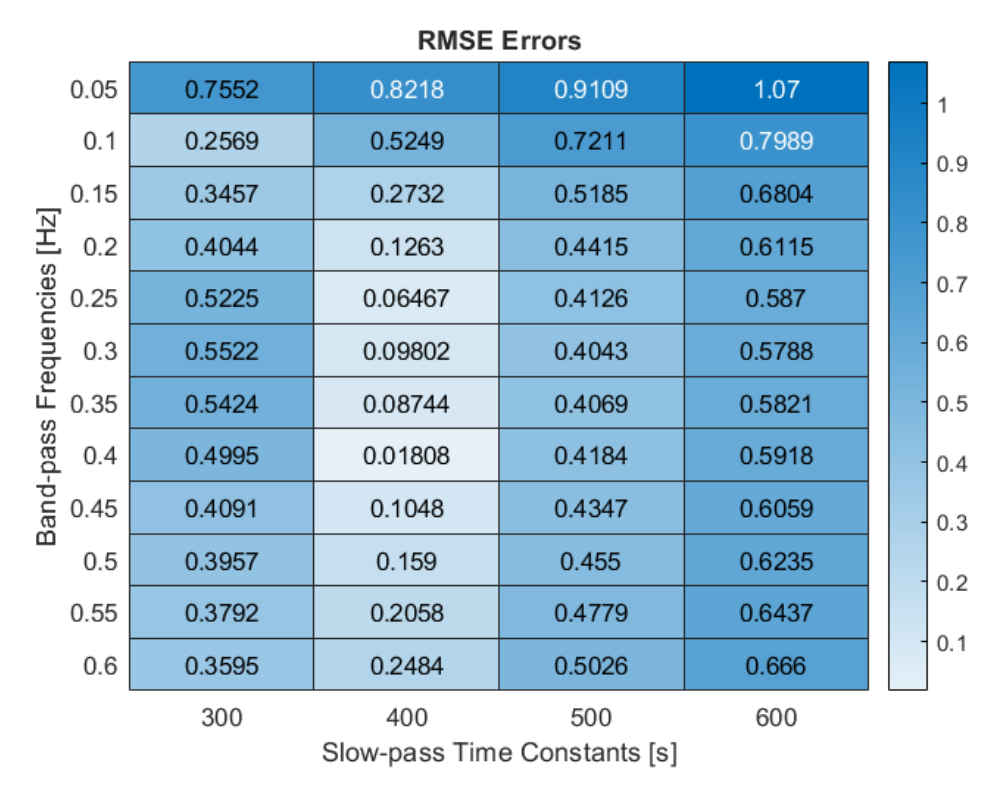


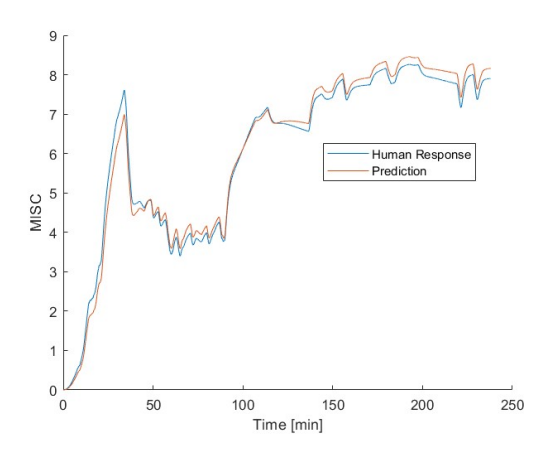
Figure 4: The heatmap of the errors using RMSE

In the heatmaps it can be seen that the SMAPE errors are very small, which slows down the algorithm due to the fact that *fmincon* has to iterate many times

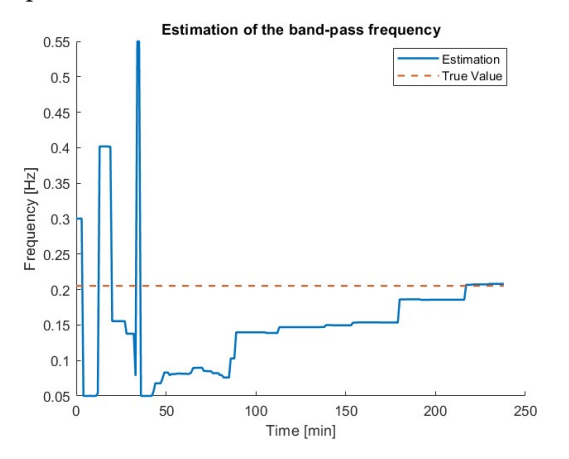
before there is an appreciable change in the error metric. Furthermore, when selecting an objective limit which is not too small, most of the parameters selected will have an error small enough to be below the objective limit. This causes the *fmincon* algorithm to choose between multiple sets of parameters, most of which are not correct. RMSE however, does have a more clear distinction between the correct and wrong parameter values. Therefore, the RMSE is chosen as the error metric which is minimized in the *fmincon* algorithm of MATLAB.

#### 2.4 Performance of the Simulation

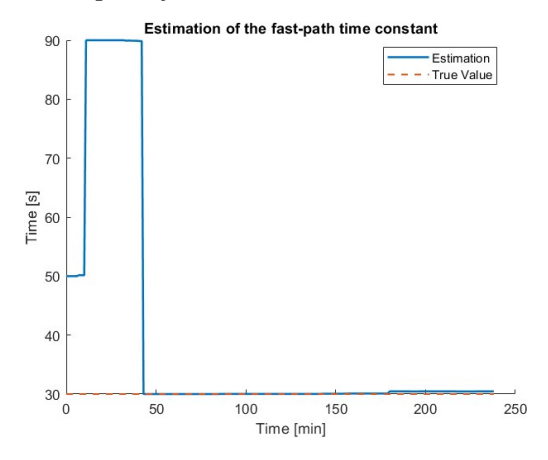
The estimation method explained in this section was simulated using MATLAB. A fictional human was simulated using the Oman model with a set of parameters generating a MISC value using an acceleration input. This output was used to estimate the set of parameters of the fictional human. The predicted MISC and the MISC of the fictional human were plotted, together with the parameters of the human against the estimated parameters to show convergence. This was done multiple times using parameters estimated from previous literature [Irmak et al., 2021]. The following plots are from a single run of the simulation.



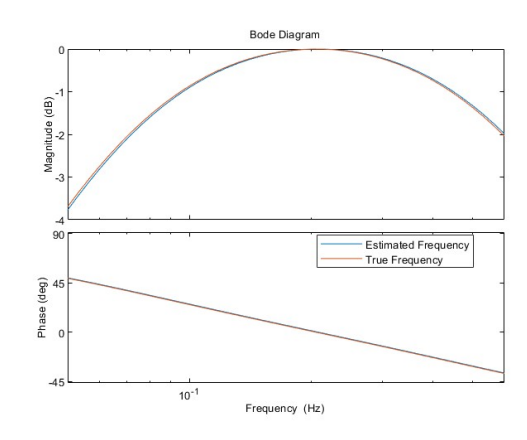
(a) The comparison between the true and estimated parameters in the Oman model for the input used in the estimation



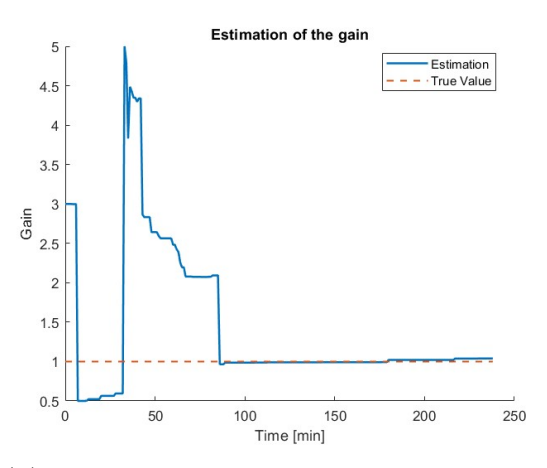
(c) The plot of the estimated and true band pass frequency



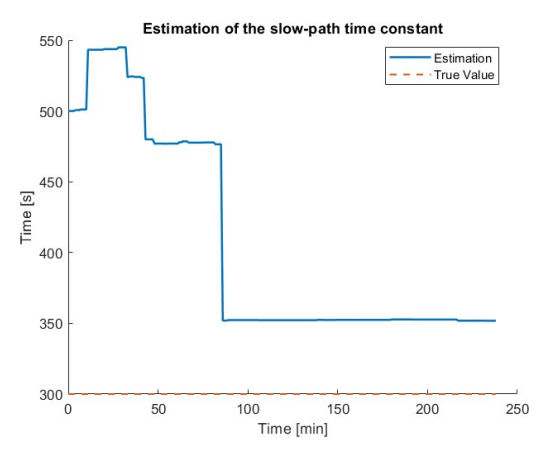
(e) The plot of the estimated and true fast path time constant



(b) The Bode plot of the estimated and true band pass frequency



(d) The plot of the estimated and true gain



(f) The plot of the estimated and true slow path time constant

Figure 5: The results of the first simulation run

## 3 Methodology

We used the estimation method developed in section 2 to subject participants to vertical accelerations of varying amplitude and frequency. There were two experimental sessions, each of 1.5 hours in duration, separated over two weeks (to reduce habituation). The repetition allowed us to quantity test-retest repeatability and the validity of the estimation method. As discussed, the aim of the experiment was to estimate individual motion sickness parameters of the expanded Oman mode (Figure 2).

#### 3.1 Ethics Statement

All participants provided written informed consent prior to participation. The experimental protocol was approved by the ethical committee of the Human Research Ethics Committee of TU Delft, The Netherlands, under application number 2772.

#### 3.2 Participants

The experiment was condicuted on 16 participants (10 male and 6 female). The participants were between 22-78 years old ( $\mu = 39.4, \sigma = 21.8$ ). Participants received a  $\in 10$  for their participation.

## 3.3 Apparatus

The experiment was conducted using the DAVSi simulator (e.g. used in [Jain et al., 2023]) [Technologies, 2021] at the 3mE faculty of TU Delft (Figure 6 and 7). This is a 6 DOF motion platform. The specifications of the simulator can be found in Figure 8. Participants were seated in the simulator, facing forwards with their eyes blinded using blackened glasses, but were asked to keep their eyes open. They were restrained to the seat using a regular seat belt and asked to sit still, without instruction regarding the hands, but the observation was that the hands rested on the legs of the participants in almost every experiment (participant 13 rested their arm in the open window). The seat back was reclined by 32 degrees (the lowest reclination of the car seat) resulting in a relaxed posture with the trunk being supported and stabilized by the back rest. The participants were asked to keep their head still against the headrest. This reduce head movements which induce coupled motions, which are more sickening. Furthermore, headphones were used reduce the perception of motion through the noise of the actuators of

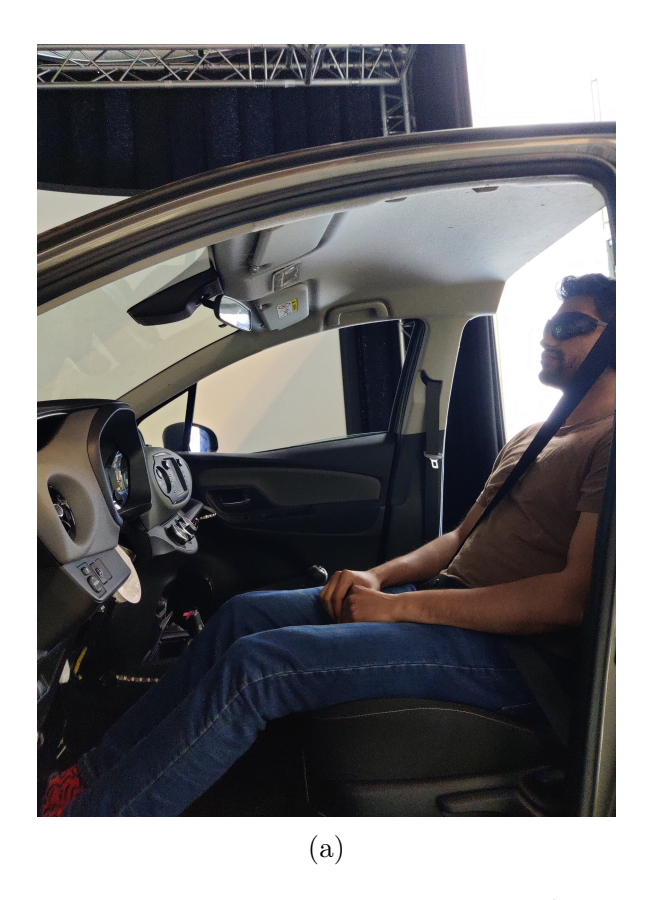




Figure 6: The participant in the simulator

the simulator, as well as give the signal to communicate their MISC rating. The MISC ratings were communicated orally.

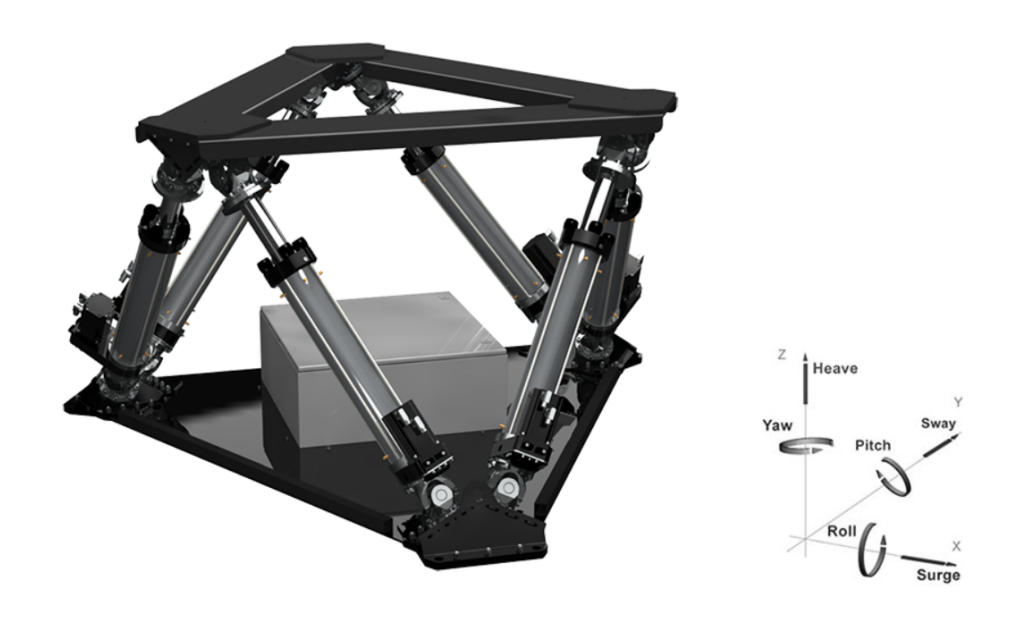


Figure 7: The DAVSi-simulator [Technologies, 2021]

Motion	Excursion [m]	Velocity [m/s]	Acceleration [m/s <sup>2</sup> ]
Surge x	-0.510.63	±0.81	±7.1
Sway y	-0.510.51	±0.81	±7.1
Heave z	-0.420.42	±0.61	±10.0
Roll $\phi$	±24.3	±35.0	±260.0
Pitch $ heta$	-25.428.4	±38.0	±260.0
Yaw $\psi$	±25.0	±41.0	±510.0
Actuator	1.2971.937	-	-

Figure 8: The specifications of the DAVSi-simulator

## 3.4 Briefing

To ensure participants knew what the experiment entailed and were adequately prepared for the experiment, every participant went through a briefing where necessary details were explained.

The participants first needed to be familiar with how they should indicate their level of sickness using the MISC scale [Bos et al., 2005], seen in Appendix B. It is key that the participants know what sickness level corresponds to what MISC rating, as otherwise the estimated level of sickness will have a systematic error. This causes the comfort when for instance adapting a route in an automated vehicle is optimized for a lower/higher sickness.

Then, the MSSQ-short form is explained and determined [Golding, 2006]. This is to see how susceptible the participants are to motion sickness and thus the representativeness with respect to population averages can be tested.

Thereafter, the participants are walked through the experiment itself, without indicating the hypotheses to prevent behaviour changes. First, the participants are made familiar with the simulator and how they are supposed to take place within, using the blinding goggles and the headphones. Then the participants are made familiar with the intercom system, where they are attended to the fact they could always stop the experiment when they feel too sick or unsafe. Last, the method of variable inputs is explained to the participants so they know what to expect from the motion stimuli.

## 3.5 Experiment

#### 3.5.1 Sickness Metrics

Motion sickness susceptibility is difficult to measure. The first attempts to quantify motion sickness susceptibility were to predict the motion sickness susceptibility of subjects with a questionnaire. [Reason and Brand, 1975] introduced the commonly used motion sickness susceptibility questionnaire (MSSQ), which was,

apart from one, the only questionnaire that was rigorously validated. This questionnaire was later revised to the MSSQ-Long [Golding, 1998]. Here, Golding simplified the scoring system, produced new reference norms for adults and investigated non-motion causes of nausea. Golding later adapted the MSSQ-Long to the MSSQ-Short [Golding, 2006], which eliminated specific questions on vomiting and excluding visual/optokinetic items due to low sickness prevalence, and they did not add significant information regarding prediction of motion sickness susceptibility. The MSSQ-Short can be seen in figure 12 in appendix A.

To determine how motion sickness develops within subjects during motion, a subjective rating scale is commonly used. This quantifies motion sickness itself, rather than motion sickness susceptibility which was just discussed. An early example is the Pensacola Motion Sickness Questionnaire (PMSQ), which links symptoms to a three-point scale to indicate the severity [Graybiel et al., 1964]. Later, the Well Being Scale (WBS) was created to have an 11-point scale [Reason and Graybiel, 1969. This had the potential to capture the progression of the motion sickness symptoms of subjects as the symptoms increase in severity from a score of 0-10. This scale however was still vague in the indication of symptoms associated with the scores. To improve the ratings associated with the scale, Bos et al. created the MIsery SCale (MISC) [Bos et al., 2005], based on the MISC which was used and validated by Wertheim et al. [Wertheim et al., 1998], where Bos et al. pooled the symptoms below nausea and gave ratings to the severity of nausea. This scale is also a 11-point scale (0-10), where 0 is zero symptoms and 10 is vomiting (see Appendix B). This scale allowed subjects to refer to the scale with their symptoms because the scale is less vague, thus increasing repeatability for subjects when they are familiarized with the scale. This scale was made by giving participants a list of symptoms associated with nausea, and were then asked to indicate which symptoms they experienced and in which order. This further supports the use of MISC for the modelling of motion sickness, as the progression is well captured with this scale. [Reuten et al., 2021] found that the MISC is more suitable than general unpleasantness ratings, as people generally rate a MISC score of 5 as more unpleasant than an MISC score of 6, while a MISC score of 6 means the motion sickness is further developed. However de Winkel et al., 2022 found the opposite to be true, thus this statement does not support the claim that the MISC rating is better than subjective discomfort.

#### 3.5.2 Procedure

Each participant was subjected twice (with a week interval) to fore-aft motions ranging between 0.05 and 0.55 Hz. This is the band of frequencies where motion

sickness occurs [O'Hanlon and McCauley, 1974]. The amplitude varied according to the formula  $KA^2 + A = 6$ , where K is the estimated gain of the Oman model. This is to ensure a response from participants who may not have a high susceptibility, and to prevent the MISC from getting to high for participants with a high susceptibility. The amplitude has a maximum of 0.25 meters as to not exceed the limits of the simulator. This limit was set by trial and error when setting up the experiment. The second experiment was done to test repeatability of the experiment. Participants who did not get sick at all in the first experiment were not asked to do the second experiment

In both experiments, the sickening motion stimuli lasted for a maximum of 1.5 hours, or until the participant reached a MISC rating of 6, indicating some nausea (see Appendix B). The acceleration amplitude and frequency are determined in intervals of 30 seconds. The participants are asked to give their MISC rating each 30 seconds via the intercom system, indicated by a beep. The indicated MISC rating is then used to estimate the new parameters of the Oman model. With the new parameters, a new input is selected. Each interval the motion fades out while the new input parameters are input in the simulator, and thereafter the motion fades in again.

## 3.6 Data Analysis

#### 3.6.1 Convergence

This study aims to test the proposed estimation algorithm, thus to see if the estimated parameters converge, each estimation iteration is shown in a plot to see if the estimation shows a convergence. In both experiments, the estimation algorithm had an end value, which are then averaged to have an average end estimation value of each parameter. This averaged end value is used to test the convergence of the algorithm. The average end estimation is subtracted from the array of estimation iterations of both experiments. The resulting arrays show the difference between each estimation iteration and the average end parameter for both experiments. Both arrays are then plotted to see how the estimation converges in both experiments.

The end values of the estimation are also compared in scatter plots to see what the difference is between the two experiments for the participants. On the x-axis, the end value of the estimation for the first experiment is represented, the second experiment is represented on the y-axis. This is also done for the RMSE of the experiments to see the difference in the model fit for both experiments.

In addition, the RMSE is shown for each iteration of the estimated parameters. Each set of parameters is used to predict the MISC from the input used in the experiment for each participant. Then, the RMSE of the response MISC and the predicted MISC is taken to see the progress of the estimation algorithm in reducing the RMSE.

#### 3.6.2 Statistical Analysis

To test if the two experiments are similar, the mean MISC of the participants is taken and tested using non-parametric tests to see if the set of means is from the same distribution. Non-parametric tests are used because the distribution is not normal when looking at the mean MISC values of the participants. To see if the distributions are different, first a box plot is made before doing the non-parametric tests.

The non-parametric tests used in this study are the Mann-Whitney U test to see if the medians of the mean MISC values are equal, and the Kruskal Wallis to see if the mean MISC values come from the same distribution.

## 4 Results

## 4.1 Course of the Experiment

Not all participants completed two sessions of the experiment. This was due to the participants not having a sickness response to the motion cues. Therefore, the second experiment was not of value for those participants who did not get sick. The MSSQ score was not part of the screening of the participants. All the participants who did not get sick had a MSSQ score of 0, except for one who had a MSSQ score of 4. However, two participants who did get sick had a MSSQ score of 2.

For the participants who completed the two sessions, a rest period of at least one week ( $\mu = 7.5 \text{ days}, \sigma = 0.99 \text{ days}$ ) was implemented as to combat habituation effects.

A point to note was that some participants got more sick in the first experiment than in the second experiment. One participant in particular reached a MISC score of 4, while in the second experiment the highest MISC was 2 and zero for a large portion of the experiment. The participant noted that in the first experiment, the motion cues were new to them and therefore they got more sick, while later in the experiment the MISC score was lower again. More participants noted that the first experiment was more sickening due to the novelty of the sickening motion for the participants. Furthermore, some participants said after the experiment that in the low frequencies, the acceleration was not noticeable, but due to the vibrations and noise of the simulator, they did get the feeling they should move, which was sickening to them.

## 4.2 Statistical Analysis

As for some participants the two experiments differed greatly, for example participant 4 and 10, the mean MISC of the participants were compared to see if they are from the same distribution. First, a box plot was made to see how the distributions compared, seen in Figure 9.



Figure 9: The box-plot of the mean MISC of both experiments

Then, two statistical tests were done on the mean of the MISC values to see if they come from the same distribution. The Mann-Whitney U test and the Kruskal Wallis test were used. The Mann-Whitney U test resulted in a p-value of 0.67 indicating the medians of the MISC values are equal at the standard 5% significance level. The Kruskal Wallis test resulted in a p-value of 0.65, indicating that the samples of the mean MISC values come from the same distribution at a 1% significance level. These tests were to see if the novelty of the sickening stimuli did not affect the response of the participants too greatly.

#### 4.3 Duration of Estimation

To reduce the amount of hours invested by participants in such experiments, an analysis is made on how long it takes for the algorithm to converge to the parameters. In the analysis, time segments are analysed by how many runs converged in that time period. Segments of 10% are chosen to analyse.

C	A 1 - 4 - 1 1
Segment	Accumulated number of converged runs
10%	0
20%	4
30%	7
40%	14
50%	15
60%	17
70%	20
80%	20
90%	20
100%	20

Table 1: The convergence in the time segments

In Table 1 it can be seen that most experiments converge within 70% of the experiment. This results in an experiment time of 63 minutes. However, not all runs converged within the 90 minutes of the experiment, as it can be seen in experiment 2 of participant 15 for example, that the Estimation of the parameters jump in the last iterations of the experiment. This did not result in a big decrease in the RMSE.

#### 4.4 Estimation of Parameters

To test the ability of the algorithm to estimate the parameters of the participants, the difference in estimation is analysed to see if the estimated parameters are precise. For each estimated parameter, the mean and standard deviation of the difference between the estimations of the first and second experiment are calculated. The plots showing the convergence of the estimated parameters of each individual can be found in Appendix C. In this section, a scatter plot of the last estimation of each parameter and the RMSE is shown. This is to see if the experiment is repeatable for the participants. A large difference in convergence in the convergence plots in the appendix can be related to the scatter plot point being off the diagonal.

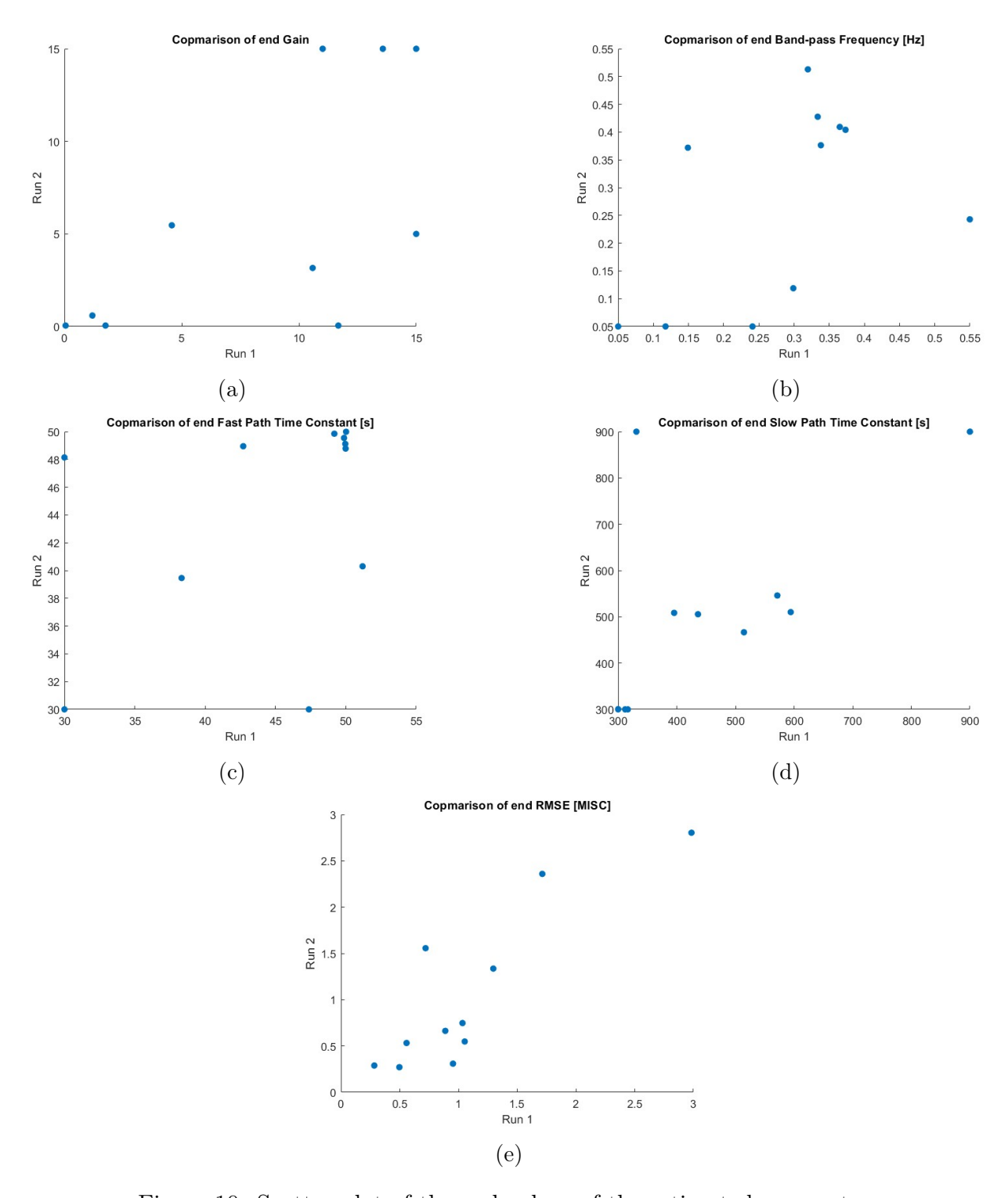


Figure 10: Scatter plot of the end values of the estimated parameters

Furthermore, in the next section the estimated parameters are compared to previous literature, to show the similarities or differences in the estimated parameters.

Parameter	$\omega$	K	$\beta_1$	$\beta_2$	RMSE
Mean	0.124	3.423	5.167	35.85	1.063
Standard Deviation	0.099	4.283	7.063	38.14	0.7911

Table 2: The mean and standard deviation of the difference of the estimated parameters

The mean differences in the estimated parameters are around 20% of the range of values for the bandpass filter frequency and gain, and 10% and 5% for the fast path time constant and slow path time constant respectively. The higher difference in the bandpass frequency and gain are partly due to a few outliers which increase the mean of the values, as the median values are much lower: 0.094 and 1.423 for the bandpass frequency and gain respectively. The participants who were the outliers in that regard had a much higher response in the first experiment compared to the second experiment. That is why the standard deviation is also high. Furthermore, the average RMSE has a high standard deviation and mean. When the outliers are removed for example, the mean and standard deviation are 0.752 and 0.389 respectively. Which is higher than the hypothesized RMSE of 0.5.

A small note to add is that the scores for the individual scores of the MSSQ did not visibly correlate with the estimated parameters. Most participants scored on the car aspect of the MSSQ-short A. But where participants had scores other than the cars, the estimated parameters did not correlate. For example, where four participants indicated they did get sick on playgrounds, the estimated parameters were not the same. One thing to note is that participant 1, 7, 15 and 16, who were the most sensitive, scored at least a 1 on the score for boats or ships.

## 5 Discussion

This study investigated whether an estimation method using optimal experiment design could estimate individual motion sickness parameters with only one experiment of 1.5 hours, significantly decreasing the time needed to model individual motion sickness resulting from sickening stimuli. The MISC ratings of participants were collected during various amplitudes and frequencies of vertical sinusoidal motion. This resulted in a predicted MISC rating for the sickening motion which the participants underwent.

#### 5.1 Performance of the Algorithm

The plots in the previous section and the appendix (Section 4.4 and Appendix C) show varying results. This depends on the difference in response over the two experiments between the same participant. When a participant shows a different response between the two experiments, the estimation of the parameters differ, for example with participant 9 and 12. Due to the nature of motion sickness, individuals can respond differently to sickening stimuli. Motion sickness can depend on various factors, such as stress or for example medication. For future research, the mood of the participants could be better monitored to try to have participants respond similarly to sickening stimuli if the research requires it, as this algorithm suffers from the different responses of the participants. Furthermore, a more robust algorithm could be designed to account for the variability in responses of participants.

The algorithm does show convergence in the RMSE, however it tries to lower the RMSE further, sometimes resulting in changes in estimated parameters after the parameters did converge. The algorithm could be adapted with a higher RMSE threshold, accounting for a higher RMSE than initially modelled, as the response of the participants could differ from the modelled response used in the simulations. This could also be due to the fact that at the lower frequencies, the acceleration was not noticeable by the participants. This was a result of the limits of the actuation of the simulator. At the lower frequencies the accelerations could not be significant as to not exceed the displacement limit. Due to the low accelerations, the algorithm predicted the MISC lower than the participants responded, resulting a higher RMSE than expected from the simulations. This could also be due to the fact that participants did find the noise and vibrations of the simulator to induce vection.

Another result of the acceleration being too low was that the algorithm cannot accurately predict the sickness response of the participants at that frequency range

(0.05 Hz to 0.15 Hz). This means that the true frequency sensitivity of the participants could lie in that bandwidth, while it could not be estimated. [O'Hanlon and McCauley, 1974] showed in the paper that the peak sensitivity of population average lies around 0.16 Hz, which means that the algorithm used in this study overestimates the peak sensitivity frequency of the participants. Future studies should use simulators, or vehicles, which can provide adequate sickening stimuli to ensure the whole bandwidth of sickening frequencies could be explored.

Lastly, the algorithm performed differently depending on how sensitive the participant was. When the participant was not sensitive, the response was zero MISC throughout the whole experiment. This meant that the response of the participants who all had zero MISC was the same, which meant the parameters could not accurately be estimated. For very sensitive participants, the algorithm did not have enough data points to estimate properly and the RMSE values were very large. This also meant the algorithm did not perform very well. For future experiments it is recommended to start the experiment with a lower amplitude (thus the initial gain estimate) to ensure participants do not get sick too quickly. The algorithm performed better for participants who did get sick, but not too quickly so the algorithm had enough data points to converge the estimated parameters.

#### 5.2 Limitations

#### 5.2.1 Q Parameter

To not make the differential equations bigger and simplify the estimation, the parameter Q (10) was assumed constant. However, in practice participants may show that they are equally sensitive to all frequencies (low Q value), or be extra sensitive to one frequency (high Q value). To test this assumption, parameters were estimated again from the input signal which was applied to the simulator and MISC response of the participants, using an extra estimation parameter in the *fmincon* algorithm of MATLAB. For the estimation after the experiment the Q could be implemented as it does not have to be differentiated for the input selection, as it had to be for the algorithm used in the experiment. This test was only the *fmincon* algorithm estimating the parameters to quickly check the validity of the assumption of the Q value.

The difference in the *fmincon* algorithm for the estimation of the Q parameter with respect to the algorithm used in the experiment was that the maximum number of iterations and function evaluations was larger for the estimation of the Q parameter. This was due to the fact that the algorithm had to estimate the parameters within 30 seconds in the experiment for it to give an input for the next 30 seconds. For the estimation of the Q parameter, the *fmincon* algorithm

also had a longer maximum allowed run time. This ensured the algorithm had a long enough run time to be able to converge better, as when the algorithm had low run time and low iterations and function evaluations, the estimation of the Q parameter was between -0.01 and 0.01 of the initial estimation.

The estimated Q parameter had a mean of 2.84, a standard deviation of 5.39 and a median of 0.17 (Figure 11). Interesting to note is that for participants who did not show a high MISC value in their response, the Q parameter was high. This is probably due to the fact that the predicted response is lower with a high Q value due to the band pass filter resulting in a low value in different frequencies.

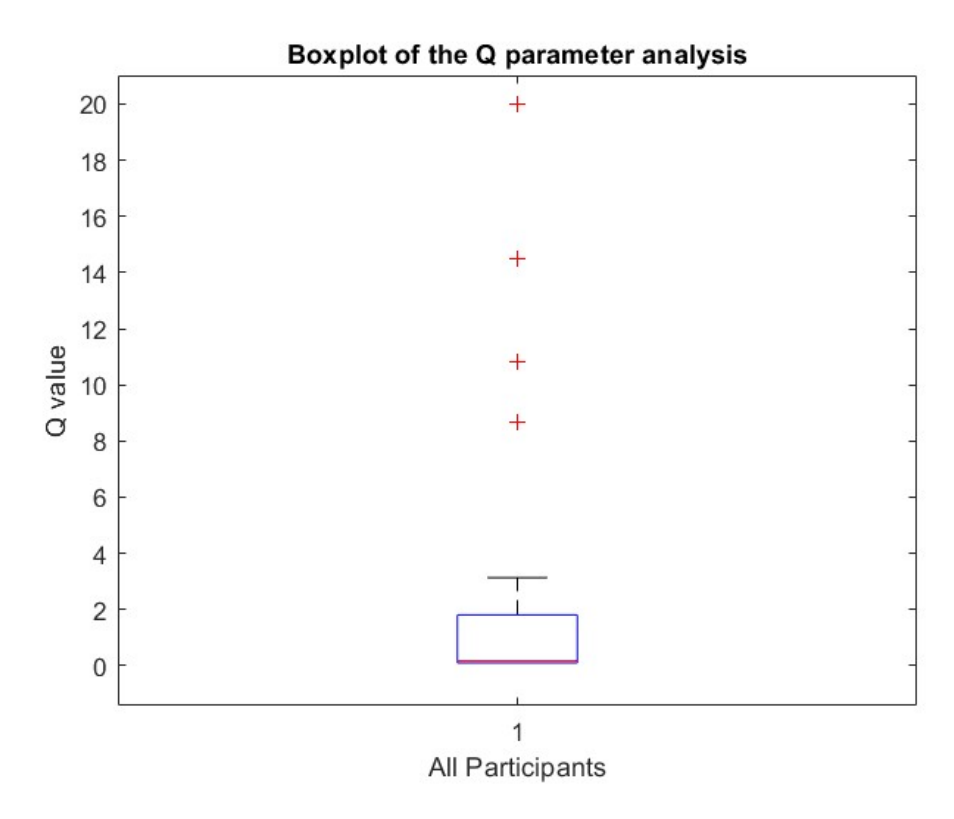


Figure 11: Boxplot of the estimated Q parameters

#### 5.2.2 Processing Power

In the algorithm, the estimation of the parameters, the selection of a new input and the setting of the new inputs in the simulator have to be done within 30 seconds. This means that the *fmincon* algorithm has limited iterations and function evaluations to estimate the parameters. Therefore, a limited amount of sets of parameters can be tested, where this amount is limited by the processing power of the computer where the algorithm runs. Increasing the processing power, or the structure of estimation could improve the accuracy of the estimation of the parameters in the experiment. This also caused the algorithm to sometimes drastically differ in the estimation of the parameters when the algorithm did not

improve on the RMSE after a long time, meaning the convergence did not always nicely show, and the RMSE did not improve either (e.g. the band pass frequency estimation in experiment 2 of participant 16).

#### 5.2.3 Simulator Limits

As discussed before, the physical limits of the simulator resulted in a very low acceleration for the low frequencies that were given as input in the algorithm. When the accelerations were low, most participants quickly reached a MISC value of zero again. The prediction of the algorithm then made the amplitude higher as to induce a response in the participants. This mostly meant that the participants had either a quick response when the frequency was higher, or a very slow response when the frequency was lower. The result was that the predicted MISC value usually was below the MISC response of the participants, as the algorithm tried to minimize the RMSE, going between the very low response and high response due to the low frequencies and higher frequencies respectively. The response therefore differed strongly from the response modelled in the simulation runs 2.4, where the MISC response increased gradually during the experiment as the low frequencies also had an adequate acceleration. Naturally this falls under the assumption that the modelled response of the participants represents the real response of the participants in an experiment.

The limits of the simulator also make that the estimated band pass frequency was not estimated in the range where the accelerations were low. Only for participants who did not get sick did the algorithm estimate a low frequency, as then the magnitude of the response was lower for all frequencies, ensuring a predicted response which was as low as possible, meaning the RMSE was lower. As the algorithm tries to minimize the RMSE, this was the reason that for the participants who did not get a MISC response higher than 0 (or 1 as seen in participant 10) the estimated band pass frequency was 0.05 Hz. Thus, for future experiment, the researcher needs to make sure that adequate sickening stimuli can be provided by the simulator, or test vehicle, such that the whole band of frequencies can be properly represented. Providing an adequate acceleration for each frequency is also to ensure that the participants do not get sick from vection. This is because some participants did get sick at the low frequencies, as they experienced vection through the vibrations and noise of the simulator. As the experiment solely focuses on the genesis of motion sickness through accelerations, vection could introduce an unwanted variable which needs to be accounted for.

Lastly, in section 4.2, the mean MISC values of the participants show that the resulting sickness from the sickening stimuli was low. This means that the resulting response is hardly sufficient to measure relevant data from the experiment.

Therefore, the results of this study mainly showcase the ability of the proposed algorithm to show convergence in the estimation of the sickness parameters of the individuals who participated in the experiment. However, the parameters themselves are not necessarily correct for the participants, as the acceleration was too low in the lower frequencies, resulting in inaccuracies in the estimation of the band pass filter frequency as discussed earlier in this section. Furthermore, the low resulting MISC means that the rest of the estimated parameters are not necessarily correctly estimated by the algorithm.

#### 5.3 Previous Literature

[Kotian et al., 2023] also models the individual parameters of the Oman model, albeit not with the frequency sensitivity of an individual modelled with a band pass filter. In the study, the range of gain values are much higher, whereas in this study the range was chosen to be smaller from the results of the literature study results. In future research, a broader range of gain values could be introduced to better model the response of participants in reality as opposed to simulation runs. Furthermore, [Kotian et al., 2023] found that the response of participants could be modelled using only two parameters in the Oman model, relating the fast path and slow path time constants to reduce computational requirements. The RMSE in the study, average of 1.1, coincide with the results seen in 2 in section 4.4. For the experiment design in this study, this would result in only 3 parameters which need to be estimated. This reduction in parameters will improve the model, as in Section 5.2.2 the limitation of the processing power is explained. It could also result in that the Q parameter could be added to the equations, resulting in a more accurate representation of the frequency sensitivity.

The relation between the gain and fast path time constant (and therefore the slow path time constant) of [Kotian et al., 2023] is also prevalent in the estimated parameters in this study. Where the gain is higher, the time constants are lower in general. However, the time constants of the fast path and the slow path do not seem to greatly affect the fit of the model.

The strength of the method used in this study is that the estimation of the parameters only needs one experiment, where the methodology of [Kotian et al., 2023] needed two datasets of experiments to estimate the sickness parameters of individuals. While the methodology in this study was using two experiments, the second experiment functioned as a control to see if the estimation of parameters was consistent over two experiments.

## 6 Conclusion

A new experiment was designed to estimate individual motion sickness parameters in a single experiment instead of multiple experiments, saving many hours of experimentation. The individual frequency sensitivity was modelled using a bandpass filter, and the sickness generation was modelled using the Oman model. The input for the model, and thus for the participants of the experiment, were sinusoidal acceleration inputs. The frequency of the sinusoidal acceleration was chosen using Fisher information, meaning the input contains the most information for the estimation of the parameters of the model. The designed experiment was able to estimate the parameters within 70% of the experiment duration, relating to 63 minutes. The average RMSE of the fit of the model was 1.06 on the MISC scale. Estimating parameters on an individual level is better to predict motion sickness in individuals than group averaged parameters. The estimated parameters were verified using a second experiment for the participants, which showed varying results depending on how similar the response was between the first and second experiment for participants.

This experiment design, with improvements, could aid in faster estimating individual motion sickness parameters, which can be used in control strategies for automated vehicles, improving the motion comfort of passengers. Furthermore, the parameters could be used in research for control strategies/motion cueing algorithms, reducing the dropout rate in experiments for example, or further research on motion sickness. The experiment design will drastically lower the time needed for experimentation for individual motion sickness parameters.

## 7 Acknowledgements

I would like to thank my supervisors, Riender Happee and Tugrul Irmak. They provided invaluable feedback, and making time to help me write the thesis despite their own time consuming projects. Furthermore, I would like to thank assistant professor Barys Shyrokau of the Cognitive Robotics department for his help in setting up the simulator. Without him, this experiment would not have taken place.

The PhD candidates at the office also provided a lot of help during the thesis process, without which I would have struggled a lot more to find a direction in which to work.

Lastly, I would like to thank my friends and family, who supported me and gave me the extra motivation to complete this project.

## References

- Bertolini, G. and Straumann, D. (2016). Moving in a moving world: A review on vestibular motion sickness. *Frontiers in Neurology*.
- Bock, O. L. and Oman, C. M. (1982). Dynamics of subjective discomfort in motion sickness as measured with a magnitude estimation method. *Aviat Space Environ Med*.
- Bos, J. E., MacKinnon, S. N., and Patterson, A. (2005). Motion sickness symptoms in a ship motion simulator: Effects of inside, outside, and no view. *Aviation Space and Environmental Medicine*.
- de Winkel, K. N., Irmak, T., Kotian, V., Pool, D. M., and Happee, R. (2022). Relating individual motion sickness levels to subjective discomfort ratings. *Experimental Brain Research*.
- Diels, C. and Bos, J. E. (2015). Self-driving carsickness. Applied Ergonomics.
- Ellis, M., Durand, H., and Christofides, P. D. (2014). A tutorial review of economic model predictive control methods. *Journal of Process Control* 24.
- Golding, J. F. (1998). Motion sickness susceptibility questionnaire revised and its relationship to other forms of sickness. *Brain Research Bulletin*.
- Golding, J. F. (2006). Predicting individual differences in motion sickness susceptibility by questionnaire. *Personality and Individual Differences* 41.
- Golding, J. F. (2016a). Motion sickness. In Furman, J. M. and Lempert, T., editors, *Neuro-Otology*, volume 137 of *Handbook of Clinical Neurology*, pages 371–390. Elsevier.
- Golding, J. F. (2016b). Motion sickness. *Handbook of Clinical Neurology*.
- Graybiel, A., Kellogg, R., and Kennedy, R. (1964). Motion sickness symptomatology of labyrinthe defective and normal subjects during zero gravity maneuvers.
- Graybriel, A. and Knepton, J. (1976). Sopite syndrome: a sometimes sole manifestation of motion sickness. *Aviat Space Environ Med*.
- Irmak, T., de Winkel, K. N., Pool, D. M., Bülthoff, H. H., and Happee, R. (2021). Individual motion perception parameters and motion sickness frequency sensitivity in fore-aft motion. *Experimental Brain Research*.
- Irmak, T., Kotian, V., Happee, R., de Winkel, K. N., and Pool, D. M. (2022). Amplitude and temporal dynamics of motion sickness. *Frontiers in Systems Neuroscience*.
- Irmak, T., Pool, D. M., and Happee, R. (2020). Objective and subjective responses to motion sickness: the group and the individual. *Experimental Brain Research*.
- Jain, V., Kumar, S. S., Papaioannou, G., Happee, R., and Shyrokau, B. (2023). Optimal trajectory planning for mitigated motion sickness: Simulator study assessment. *IEEE Transactions on Intelligent Transportation Systems*, pages 1–12.
- Jauberthie, C., Bournonville, F., Coton, P., and Rendell, F. (2005). Optimal input design for aircraft parameter estimation. *Aerospace Science and Technology* 10.
- Keshavarz, B., Hecht, H., and Lawson, B. (2014). Visually induced motion sickness: Characteristics, causes, and countermeasures, pages 648–697.
- Kotian, V., Pool, D. M., and Happee, R. (2023). Modelling individual motion sicnkess accumulation in vehicles and driving simulators. *DSC 2023 Europe*.
- Kufver, B. and Förstberg, J. (1999). A net dose model for development of nausea. *United Kingdom Group Meeting on Human Responses to Vibration*.
- Kuiper, O. X., Bos, J. E., Diels, C., and Schmidt, E. A. (2020). Knowing what's coming: Anticipatory audio cues can mitigate motion sickness. *Applied Ergonomics*.
- Lackner, J. R. (2014). Motion sickness: more than nausea and vomiting. Exp Brain Res.

- Litman, T. (2022). Autonomous vehicle implementation predictions: Implications for transport planning. Victoria Transport Policy Institute.
- Matsangas, P., McCauley, M. E., and Becker, W. (2014). The effect of mild motion sickness and sopite syndrome on multitasking cognitive performance. *Human Factors*.
- Mueller, A. S., Cicchino, J. B., and Zuby, D. S. (2020). What humanlike errors do autonomous vehicles need to avoid to maximize safety? *Journal of Safety Research*.
- O'Hanlon, J. and McCauley, M. (1974). Motion sickness incidence as a function of the frequency and acceleration of vertical sinusoidal motion. *Human Factors Research*.
- Oman, C. M. (1990). Motion sickness: a synthesis and evaluation of the sensory conflict theory. Can. J. Physiol. Phamcol.
- Qian, J., Nadri, M., and Dufour, P. (2016). Optimal input design for parameter estimation of nonlinear systems: case study of an unstable delta wing. *International Journal of Control*.
- Rawlings, J. B., Angeli, D., and Bates, C. N. (2012). Fundamentals of economic model predictive control. 51st IEEE Conference on Decision and Control.
- Reason, J. T. (1978). Motion sickness adaptation: a neural mismatch model. *Journal of the Royal Society of Medicine*.
- Reason, J. T. and Brand, J. J. (1975). Motion Sickness. London: Academic Press.
- Reason, J. T. and Graybiel, A. (1969). Changes in subjective estimates of well-being during the onset and remission of motion sickness symptomatology in the slow rotation room. *Naval Aerospace Medical Institute vol 1083*.
- Reuten, A. C., Nooij, S. A. E., Bos, J. E., and Smeets, J. B. J. (2021). How feelings of unpleasantness develop during the progression of motion sickness symptoms. *Experimental Brain Research*.
- Riccio, G. E. and Stoffregen, T. A. (1991). An ecological theory of motion sickness and postural instability. *Ecological Psychology*.
- SAE International (2014). Taxonomy and definitions for terms related to driving automation systems for on-road motor vehicles.
- Singh, S. (2018). Critical reasons for crashes investigated in the national motor vehicle crash causation survey. *Traffic Safety Facts Crash Stats*.
- Smyth, J., Jennings, P. A., Mouzakitis, A., and Birrell, S. A. (2018). Too sick to drive: How motion sickness severity impacts human performance. 2018 21st International Conference on Intelligent Transportation Systems (ITSC).
- Stoffregen, T. A. and Smart, J. L. (1998). Postural instability precedes motion sickness. *Brain Research Bulletin*.
- Takov, V. and Tadi, P. (2019). Motion Sickness. StatPearls Publishing.
- Talsma, T. M., Hassanain, O., Happee, R., and de Winkel, K. N. (2023). Validation of a moving base driving simulator for motion sickness research. *Applied Ergonomics*.
- Technologies, E. (2021). Em6-400-1500.
- Wertheim, A. H., Bos, J. E., and Bles, W. (1998). Contributions of roll and pitch to sea sickness. Brain Research Bulletin.

## Appendix

## A MSSQ

Motion sickness susceptibility questionnaire short-form (MSSQ-Short)

This questionnaire is designed to find out how susceptible to motion sickness you are, and what sorts of motion are most effective in causing that sickness. Sickness here means feeling queasy or nauseated or actually vomiting

Your childhood experience only (before 12 years of age), for each of the following types of transport or entertainment please indicate

1. As a child (before age 12), how often you felt sick or nauseated (tick boxes)

	Not Applicable - Never	Never Felt Sick	Rarely Felt Sick	Sometimes Felt Sick	Frequently Felt Sick
	Traveled				
Cars					
Buses or Coaches					
Trains					
Aircraft					
Small Boats					
Ships, e.g. Channel Ferries					
Swings in playgrounds					
Roundabouts in playgrounds					
Big Dippers, Funfair Rides					
	t	0	1	2	3

Your experience over the last 10 years (approximately), for each of the following types of transport or entertainment please indicate

2. Over the last 10 years, how often you felt sick or nauseated (tick boxes)

	Not	Never	Rarely	Sometimes	Frequently
	Applicable	Felt Sick	Felt Sick	Felt Sick	Felt Sick
	- Never				
	Traveled				
Cars					
Buses or Coaches					
Trains					
Aircraft					
Small Boats					
Ships, e.g. Channel Ferries					
Swings in playgrounds					
Roundabouts in playgrounds					
Big Dippers, Funfair Rides					
	t	0	1	2	3

Figure 12: The MSSQ-Short from [Golding, 2006]

## B MISC

Symptom  No problems  Slight discomfort but no specific symptoms							
					Dizziness, warm, headache, stomach awareness, sweating, etc.	vague some medium severe	2 3 4 5
					Nausea	some medium severe retching	6 7 8 9

Figure 13: The Misery Scale (MISC) [Bos et al., 2005]

C Convergence of Parameters

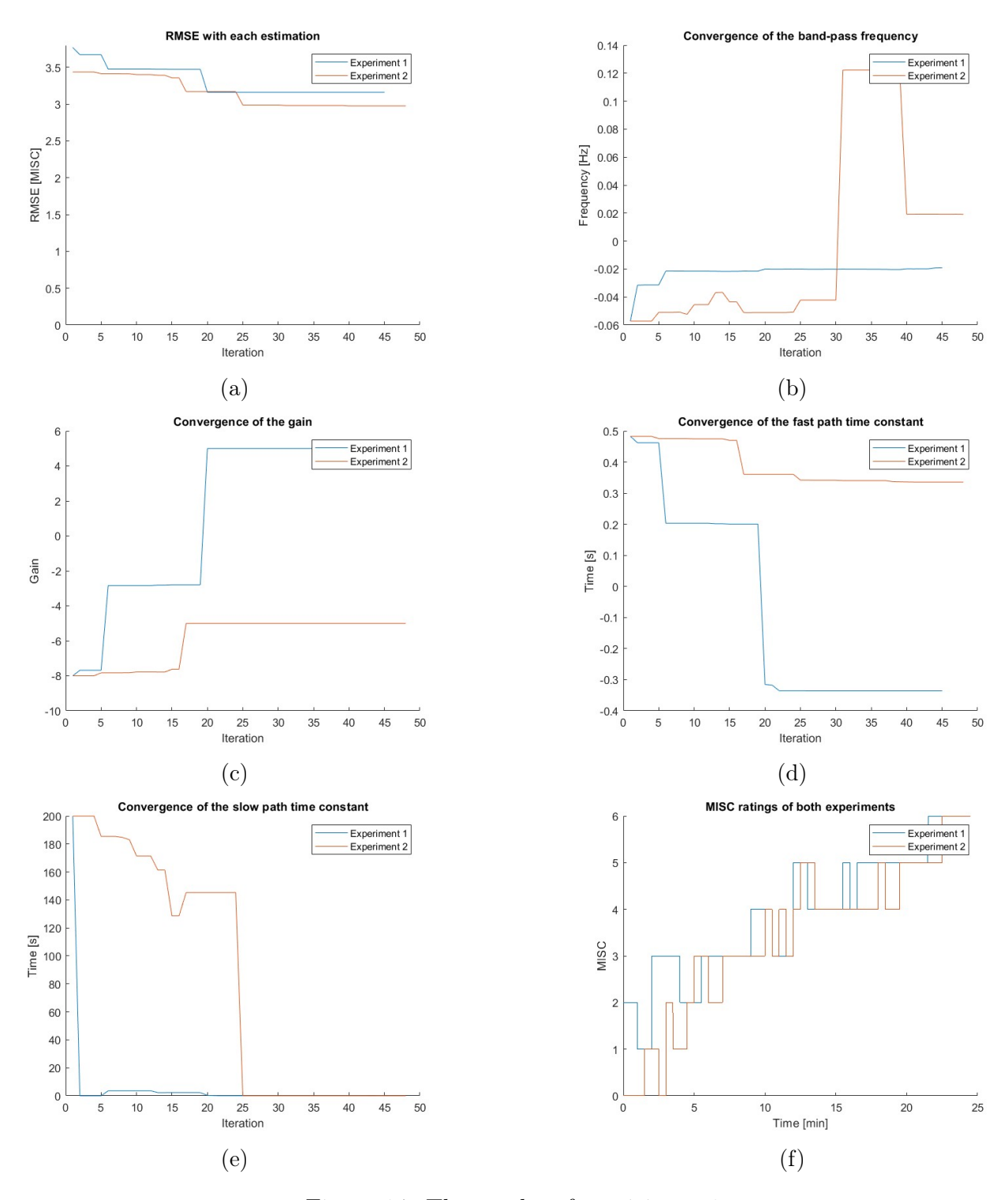


Figure 14: The results of participant 1

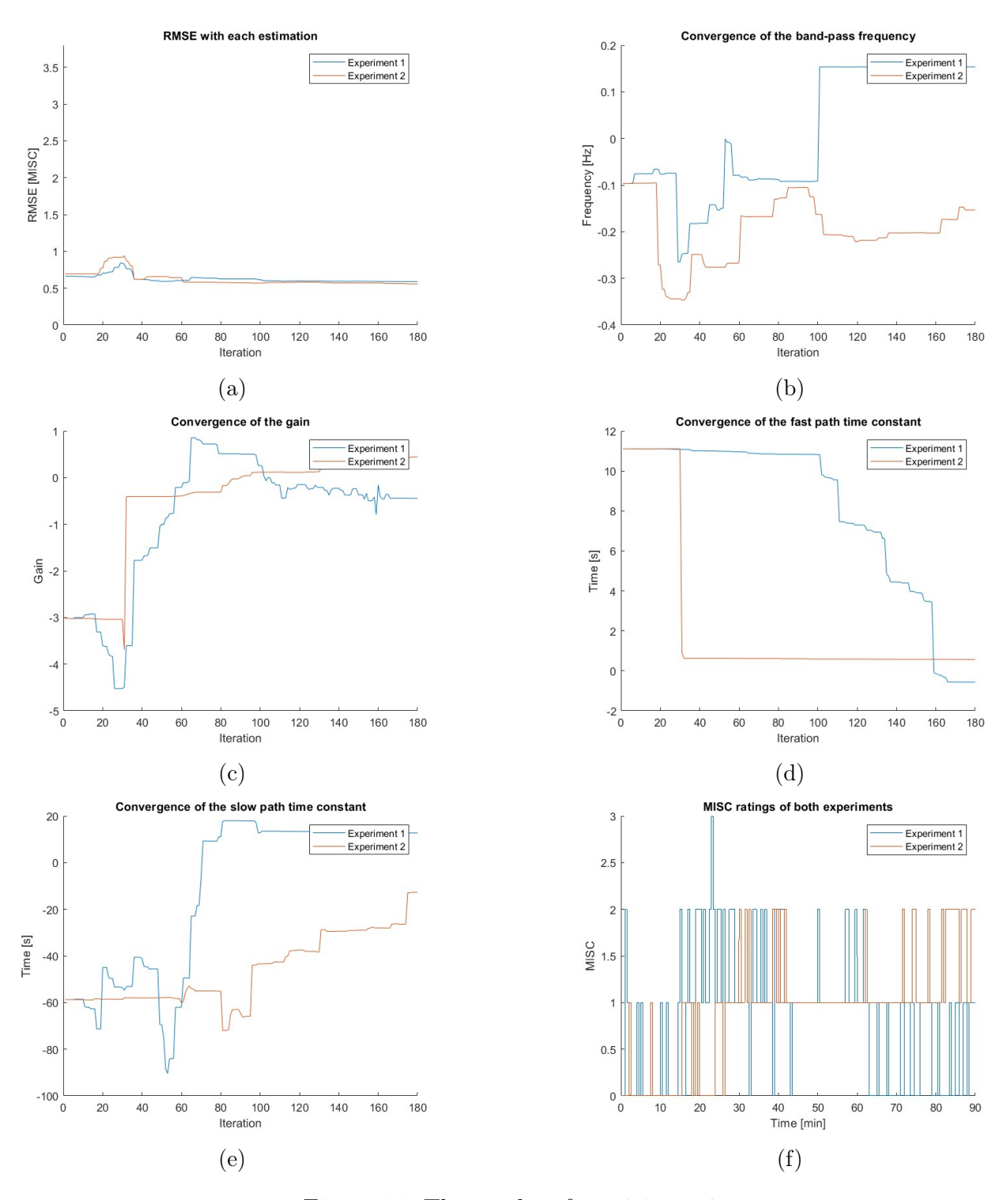


Figure 15: The results of participant 2

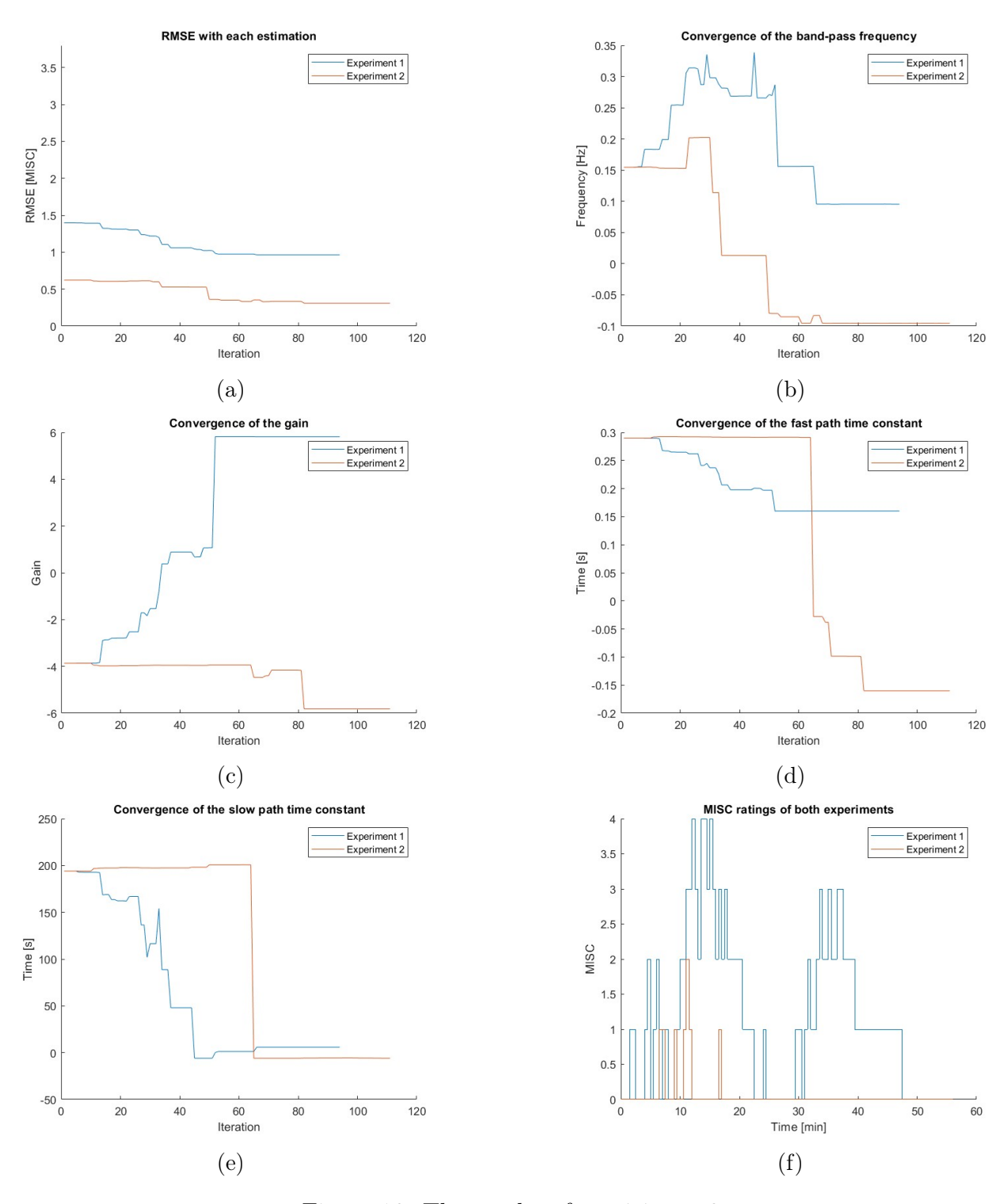


Figure 16: The results of participant 6

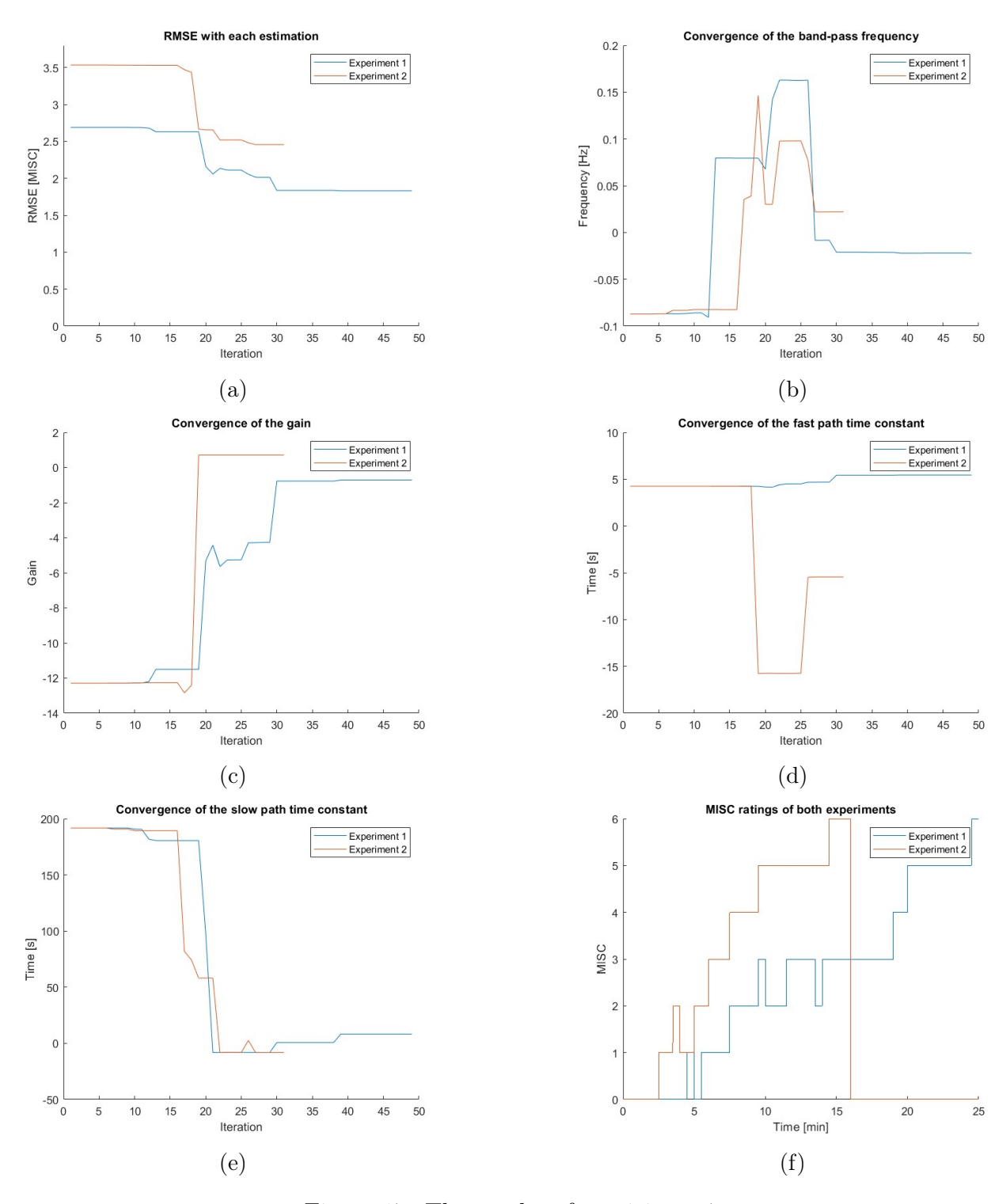


Figure 17: The results of participant 7

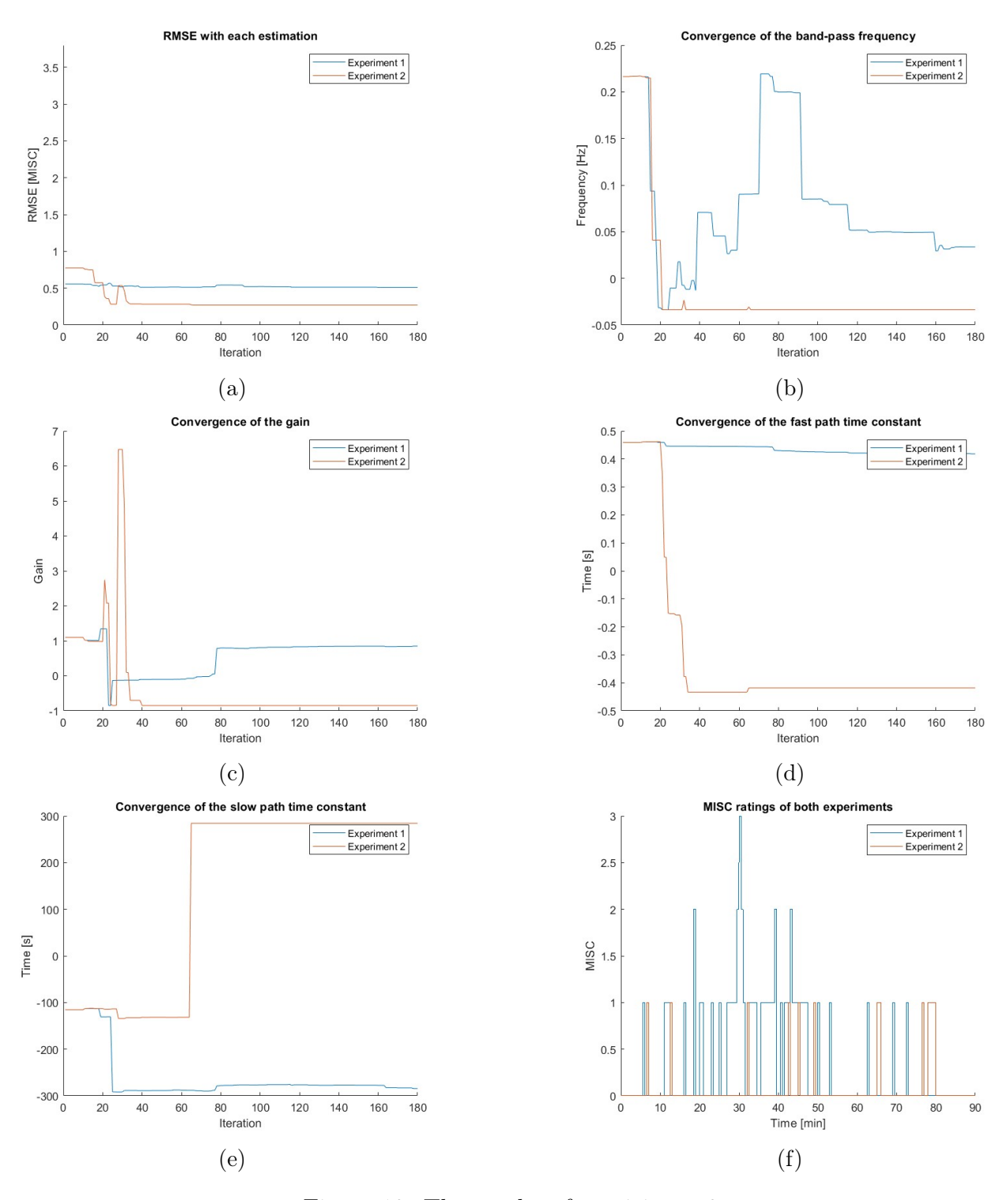


Figure 18: The results of participant 8

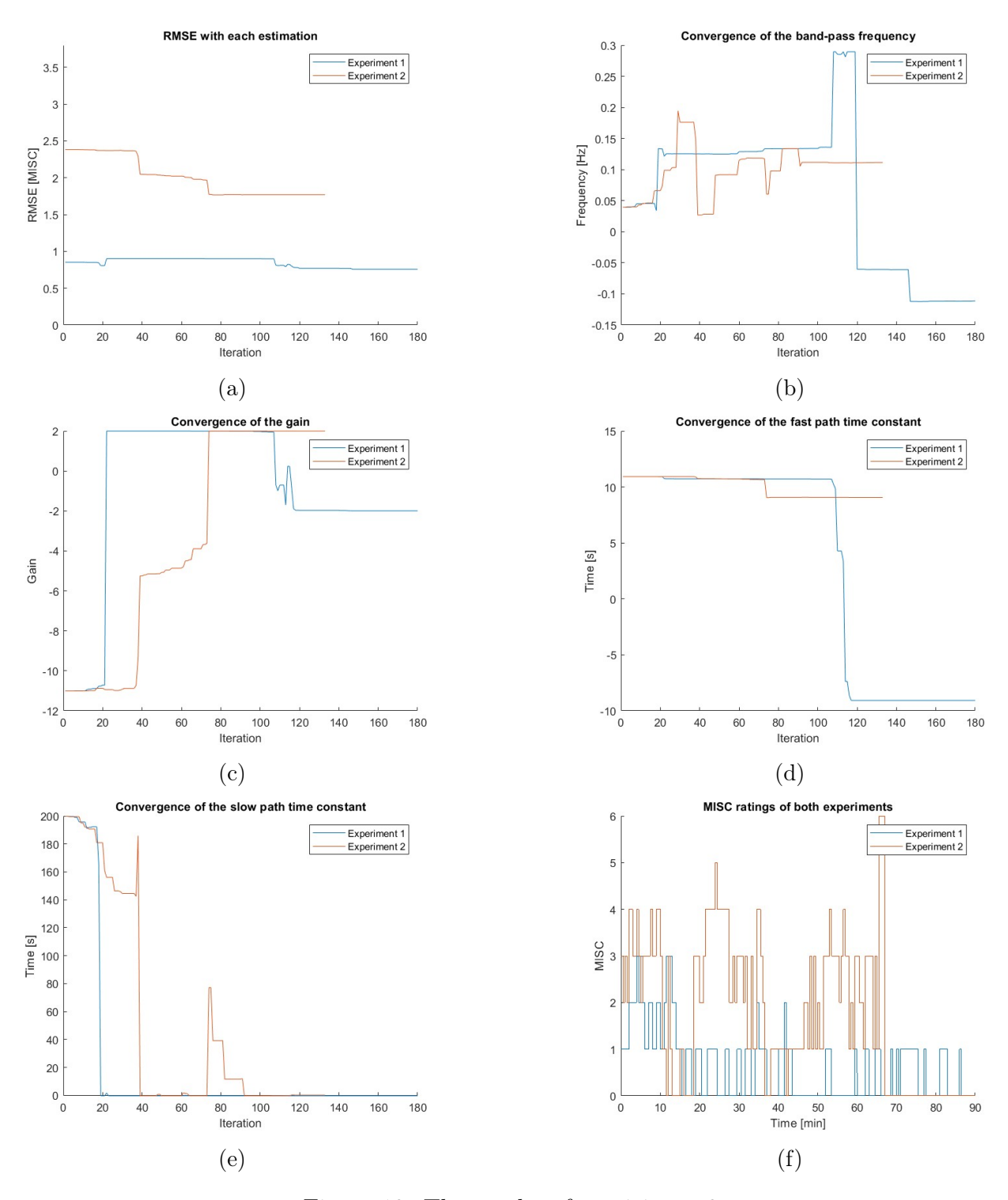


Figure 19: The results of participant 9

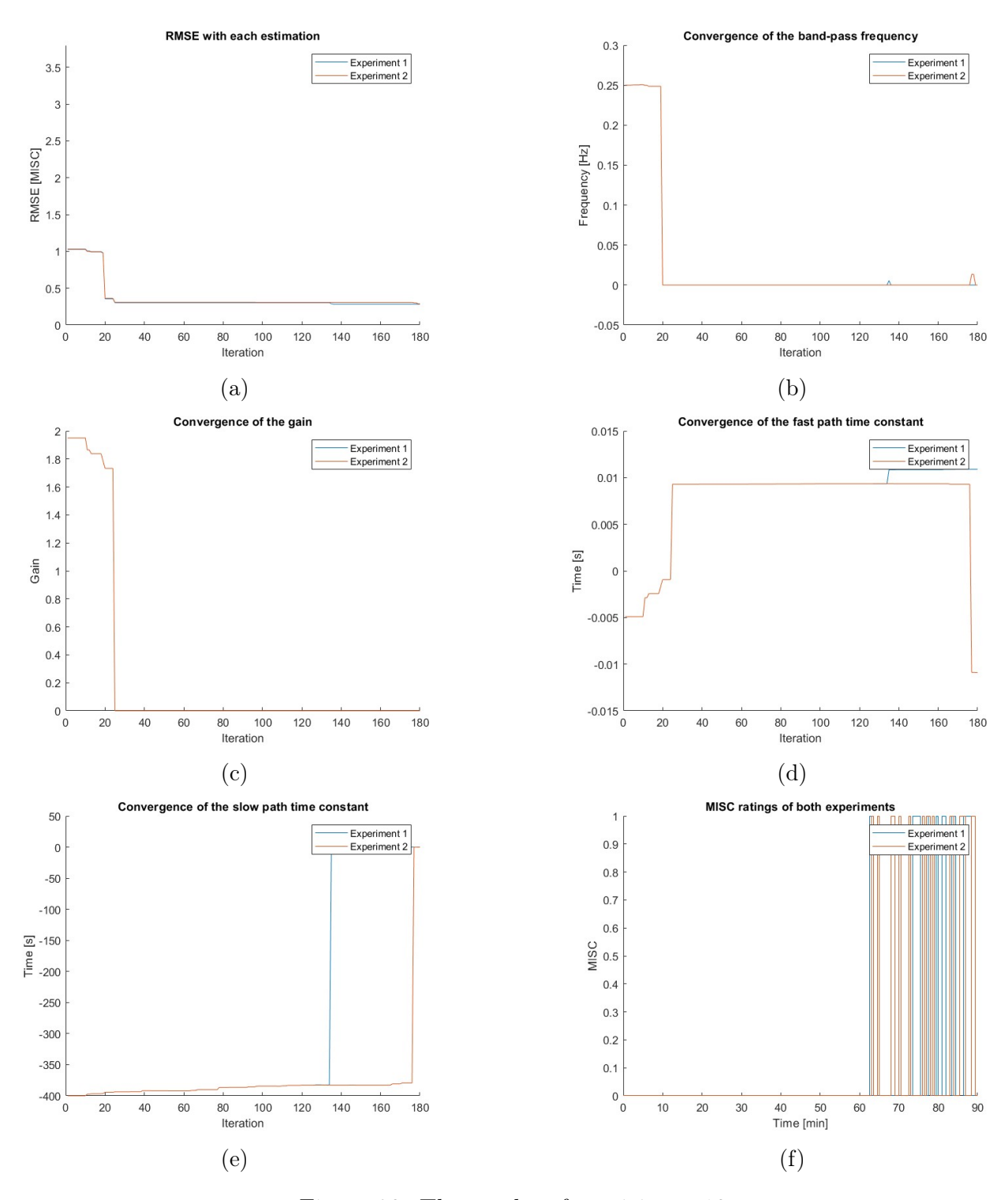


Figure 20: The results of participant 10

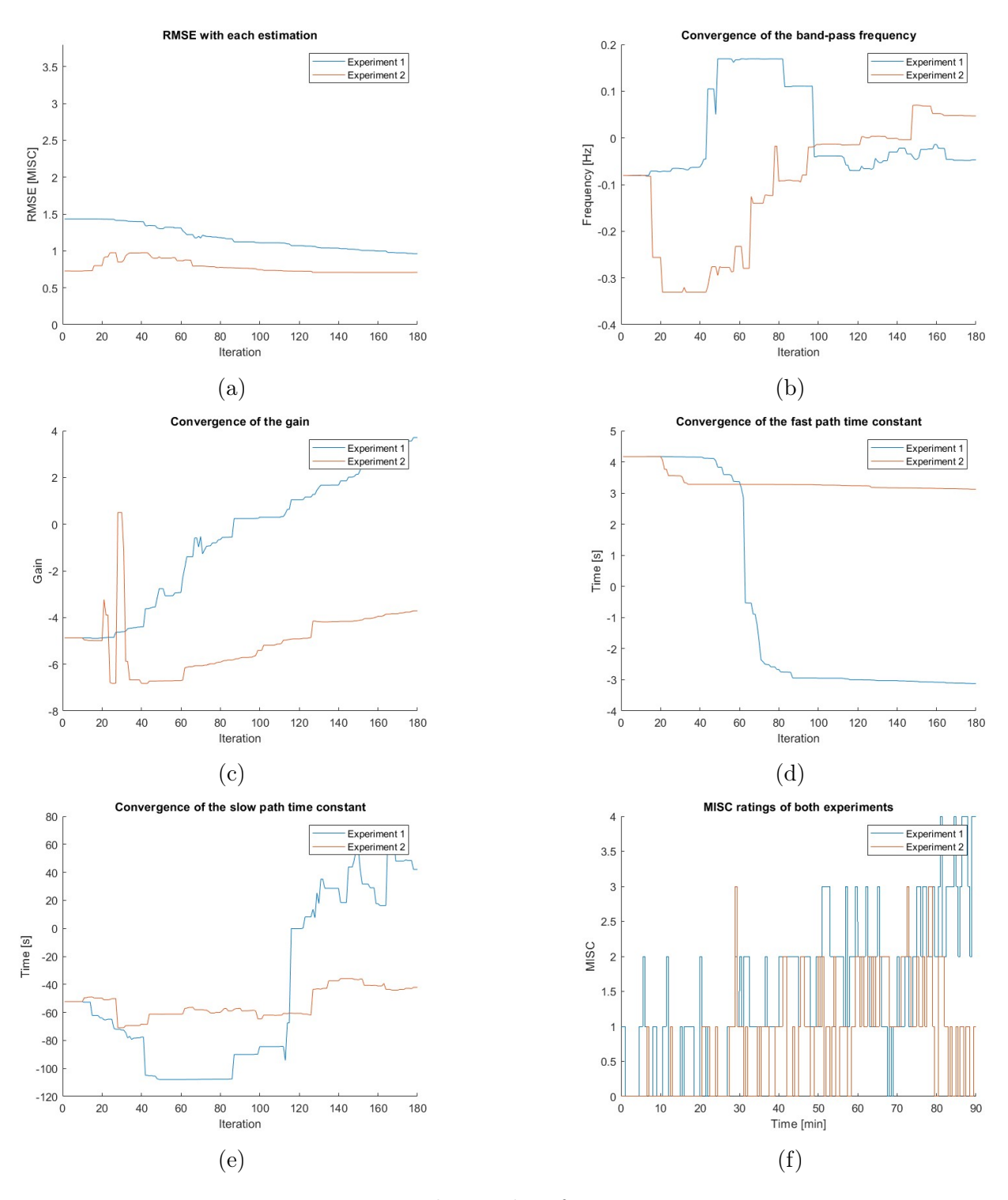


Figure 21: The results of participant 11

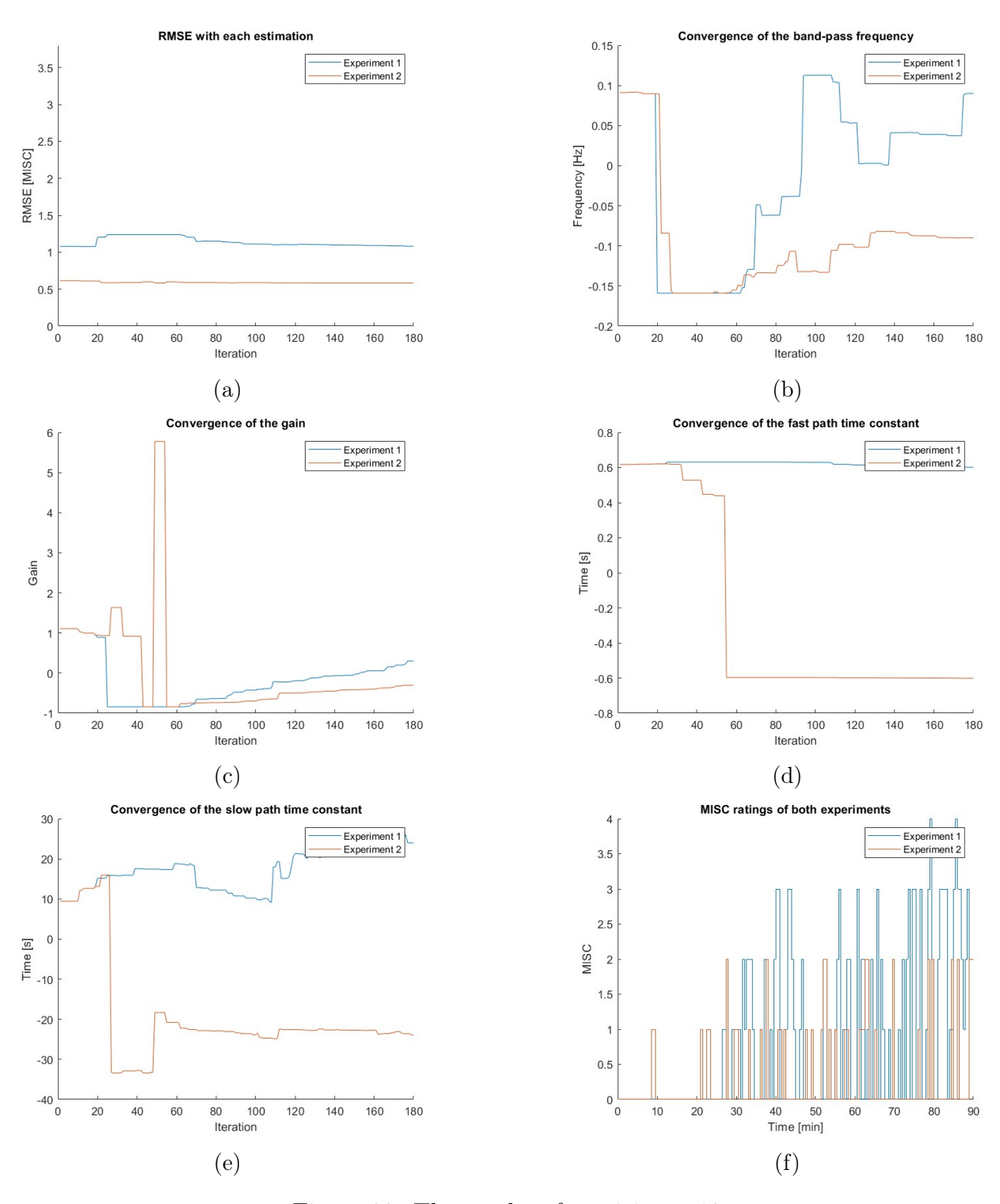


Figure 22: The results of participant 12

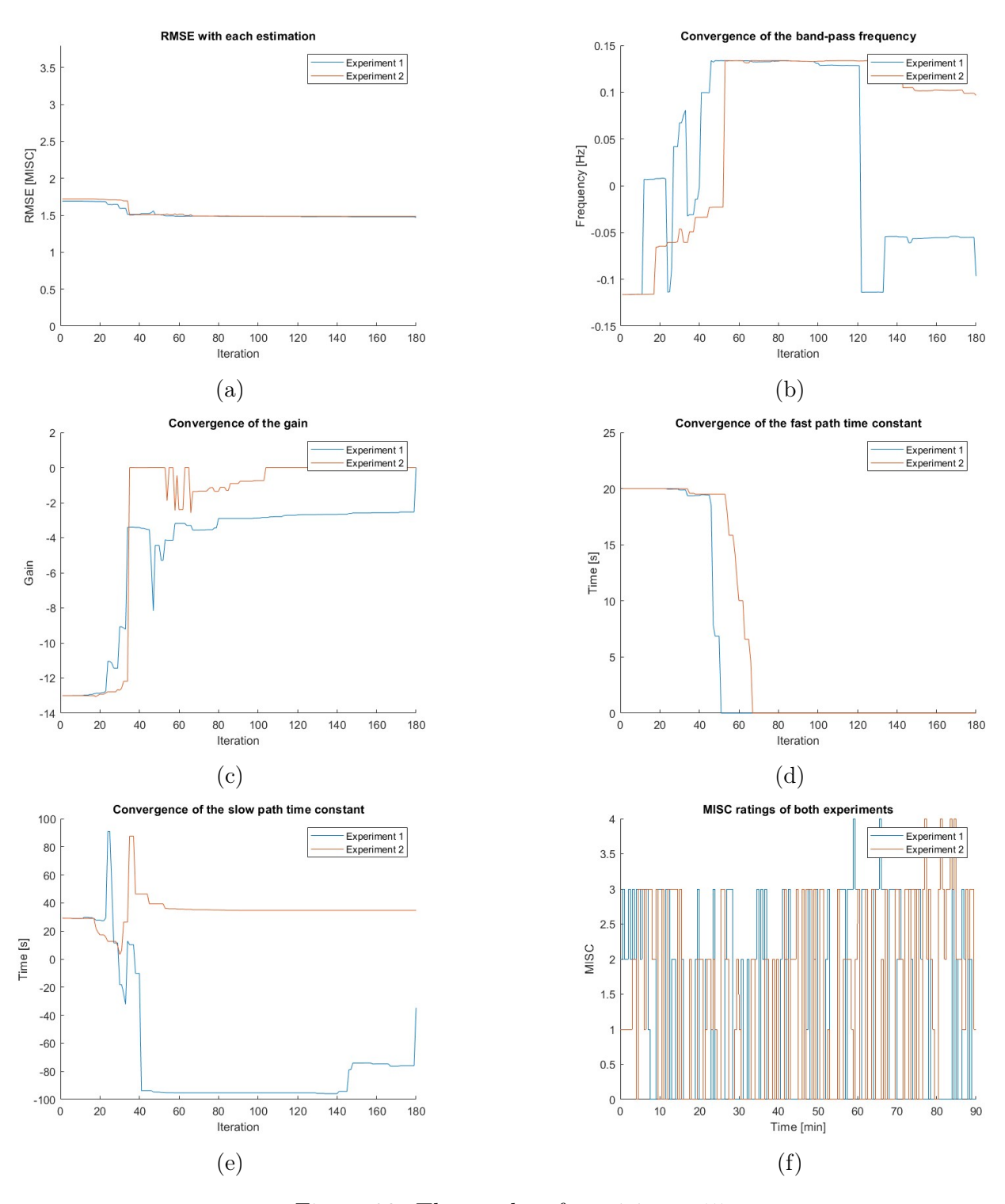


Figure 23: The results of participant 15

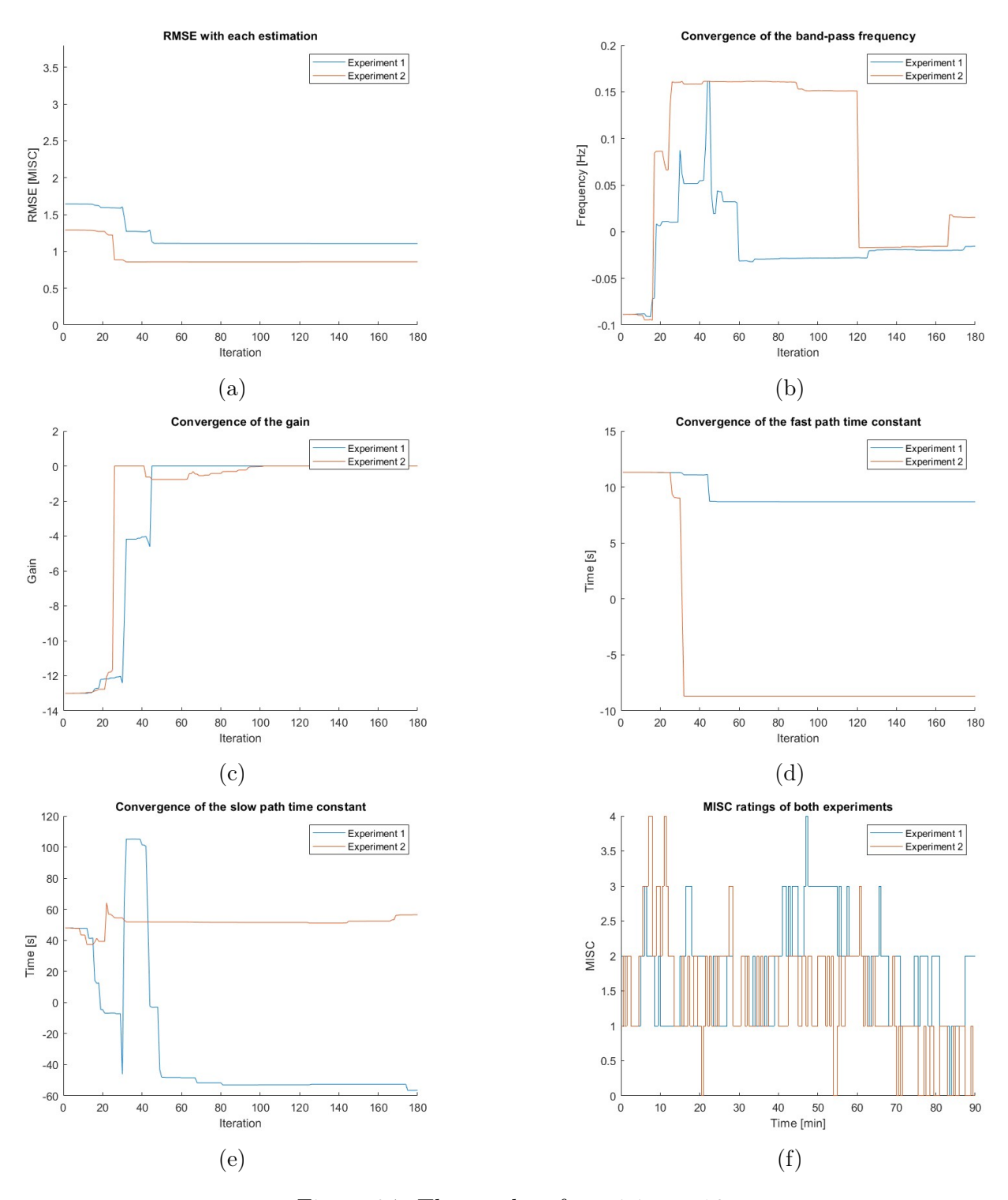


Figure 24: The results of participant 16